

Chapter 2

Centred Axial Force

Abstract This chapter presents the design methods of reinforced concrete elements subjected to axial action, starting from the columns under compression and proceeding with the tension members, for which in particular the criteria for cracking calculation are given. In the final section the structure of a multi-storey building is described, assumed as applicative example for the design calculations. The analysis of loads is developed and the complete design of a column is shown.

2.1 Compression Elements

Reinforced concrete columns have two types of reinforcement (see Fig. 2.1): longitudinal reinforcement consisting of bars at the corner and possibly also on the long sides; transverse reinforcement consisting of stirrups, which are bars of smaller diameter shaped to enclose the longitudinal reinforcement.

Under compression actions that are essentially centred, no tensile stresses arise in the columns. One could therefore think of not adopting any reinforcement at all, as concrete resists compression well. However, its brittleness requires a remedial. If massive works are excluded, for which any possible local brittle damage has a small impact on the global resistance, concrete elements always have to be encased in a sort of superficial steel cage. The size of such steel cage has to be related to the mass of concrete to be reinforced in order to introduce a significant increase in ductile resistance. This leads to *minimum reinforcement* requirements such as

$$A_s \geq \rho_o A_c$$

which imposes a minimum value ρ_o (e.g. =0.003) to the longitudinal *reinforcement geometrical ratio* $\rho_s = A_s/A_c$; or such as

The original version of this chapter was revised: For detailed information please see Erratum. The erratum to this chapter is available at [10.1007/978-3-319-52033-9_11](https://doi.org/10.1007/978-3-319-52033-9_11)

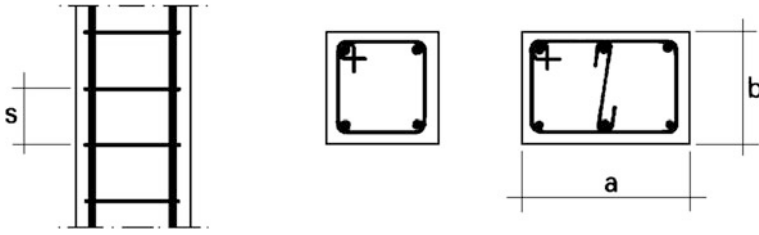


Fig. 2.1 Details of RC column—view and sections

$$A_s \geq v_0 N_{Ed}/f_{sd}$$

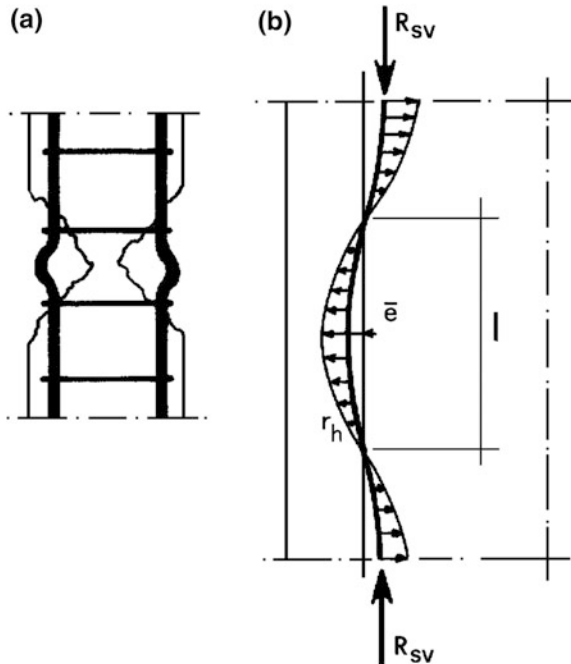
which imposes the possible increase in reinforcement based on a minimum ratio v_0 (e.g. ≈ 0.10) of the expected load.

Furthermore, an adequate distribution of reinforcement has to be guaranteed, imposing a *maximum spacing* of bars (e.g. ≤ 300 mm) and correlating the spacing of stirrups to the column smaller side (e.g. $s \leq b$).

For reinforcement lower than the minimum values mentioned above, one can refer to the typology of *plain concrete* works (unreinforced or with light reinforcement), such as walls and other massive structures, designed according to specific criteria.

High reinforcement ratios, greater than a limit ρ_1 of about 4%, make the effective collaboration between the two materials uncertain because of bond problems. When

Fig. 2.2 Buckling of bars in compression



the steel area is higher than the mentioned limit, one enters a range of a different type of composite material. One then refers to *composite structures*, where bond between steel and concrete should rely on special connecting devices and not only to surface adhesion.

The failure mode of a column in compression is indicated in Fig. 2.2a, with the development of the typical “hourglass” shape in the concrete and with buckling of the longitudinal reinforcement. From this failure mode another important function of the stirrups is deduced, which is the limitation of the buckling length of the longitudinal bars, which otherwise would be too instable to offer a significant contribution to resistance. The *maximum spacing* of stirrups therefore has to be related to the diameter of the longitudinal bars with limitations such as

$$s \leq \kappa_o \phi$$

which, for example, with $\kappa_o = 12$, (being $i = \phi/4$ the radius of gyration and $s_o = 0.5 s$ the buckling length), implicitly impose the limit

$$\lambda = s_o/i = 24$$

to the slenderness of the bars.

The stirrups have to be shaped and sized to guarantee an *effective restraint* towards the inside of the column, working in tension. Given that the transverse restraining force is proportional to the vertical one that runs inside the longitudinal bars (e.g. a few percent), the diameter of the stirrups has to be correlated to the one of the longitudinal reinforcement with limitations such as $\phi' \geq \phi/n$. The presence of longitudinal bars on the sides requires the addition of specific transverse connecting links.

The two *ends of the column* are the most critical zones, because of the possible disturbance created by the bars lapping (usually at the bottom), and because the bending moment reaches its maximum values there. It is good practice to reduce the stirrups spacing in those zones, for example halving it, in order to enhance their confining effect.

The reinforcement of elements with elongated cross section, such as *walls* (see Fig. 2.3a), requires the introduction of two sets of bars close to the external surfaces. The reinforcement consisting of horizontal straight bars of smaller diameter does not offer the through-link required to restrain the vertical bars with tensile forces only. For this, appropriate links (similar to the one shown with a dashed line in the figure) would be necessary, one for each pair of vertical bars, spaced vertically according to the same criteria described for stirrups.

Links are not necessary if the concrete layer covering the vertical bars can restrain them with transverse tensile stresses σ_h (see Fig. 2.3b). These tensile stresses should be low enough so that the concrete resistance to the vertical compressions is not significantly reduced. This leads to limitations for the diameter ϕ of the bars with respect to the concrete cover c . Only short notes are hereby given about the criterion that gives such limitations, as the numerical results are based on some parameters that are difficult to quantify.

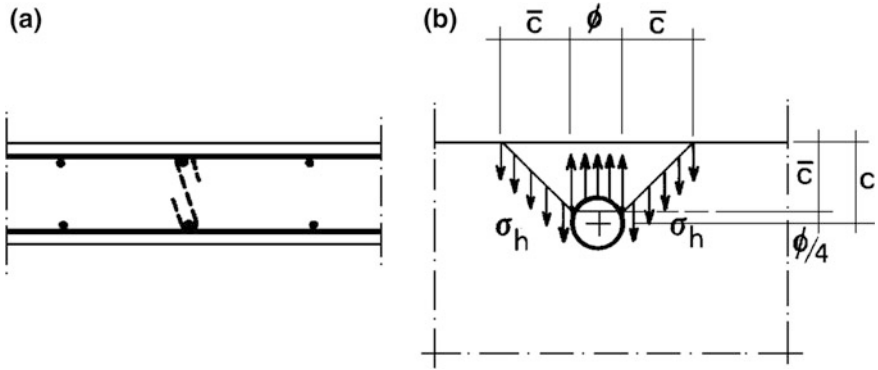


Fig. 2.3 **a** Transverse links and **b** restraint mechanism

Assuming a conventional model for the profile of the vertical bars to represent straightness tolerances of the bars, for example with the sinusoidal function (see Fig. 2.2b):

$$e = \bar{e} \sin \frac{\pi}{l} x$$

under the action of the vertical force R_{sv} a transverse reaction is generated which varies according to the second-order derivative of the profile

$$r_h \cong R_{sv} e''$$

This reaction is able of resisting the vertical force without relying on the bending stiffness of the bar. The maximum value of the horizontal force coincides with the point of maximum curvature $\bar{\chi}$ and can be expressed as inversely proportional to the diameter. At the yield limit of the bar, one therefore has

$$\bar{r}_h = A_s f_y \bar{\chi} = \frac{\pi \phi^2}{4} f_y \frac{\kappa}{\phi}$$

The tensile stresses σ_h in the concrete cover oppose to the deviating action of the bar (see Fig. 2.3b), according to the equilibrium

$$\bar{r}_h = 2\bar{c}\sigma_{ct}/\sqrt{2}$$

Imposing the limit $\leq \beta f_{ct}$ (for example with $\beta = 0.20$) to such tension, it is eventually deduced

$$\bar{c} \geq 0.125 \sqrt{2} \pi \frac{\kappa f_y}{\beta f_{ct}} \phi$$

where, with $f_y/f_{ct} \cong 250$, the tolerance κ has to be appropriately estimated. If, for example $\kappa = 1/400$ is assumed, the *minimum cover* is obtained with

$$c \geq \frac{\phi}{4} + \bar{c} \cong 2\phi$$

as a function of the diameter of the longitudinal bar, in order to rely on the full strength of the materials without the need for transverse confining links.

2.1.1 Elastic and Resistance Design

Given the reinforced concrete section of Fig. 2.4 subject to a centred compression force N , for the first design assumption the section translates remaining plane, exhibiting a constant contraction ε under load. For the second assumption of perfect bond between the two materials, it derives that steel is subject to the same deformation $\varepsilon_s = \varepsilon_c = \varepsilon$. The third assumption of concrete cracking in tension does not come into play, since only compression stresses occur: the resisting section in this case coincides with the geometrical section.

For an *elastic design*, stresses in the two materials are therefore obtained with the Hooke's law:

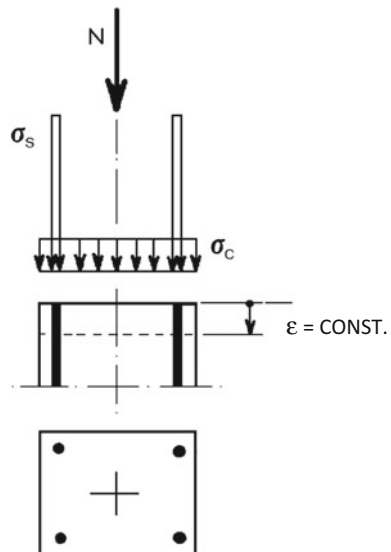
$$\sigma_c = E_c \varepsilon_c = E_c \varepsilon$$

$$\sigma_s = E_s \varepsilon_s = E_s \varepsilon$$

where in particular, for the equality of deformations ε , one has:

$$\frac{\sigma_c}{E_c} = \frac{\sigma_s}{E_s}$$

Fig. 2.4 Stresses on the section



which leads to

$$\sigma_s = \alpha_e \sigma_c$$

where $\alpha_e = E_s/E_c$ is the ratio between the elastic moduli of the two materials.

The equilibrium to translation of the cross section is therefore set with

$$\sigma_c A_c + \sigma_s A_s = N$$

having indicated with A_c and A_s the areas of concrete and steel, respectively, affected by stresses σ_c and σ_s . Introducing the above-mentioned relationship between these stresses, one eventually obtains:

$$\sigma_c (A_c + \alpha_e A_s) = \sigma_c A_i = N$$

having set

$$A_i = A_c + \alpha_e A_s$$

equivalent area of the section equalized to concrete. That is, in the elastic range, the steel area A_s should be amplified with the *homogenization coefficient* α_e to obtain a concrete area of the same capacity.

Indicating with ψ_s the *reinforcement elastic ratio*, evaluated weighing the areas of the two materials with the respective elastic moduli

$$\psi_s = \frac{E_s A_s}{E_c A_c} = \alpha_e \rho_s$$

one can express

$$A_i = A_c (1 + \psi_s)$$

where the amplification factor of the concrete area is enclosed in brackets.

The value of stresses under a given force N is therefore deduced as:

$$\begin{aligned} \sigma_c &= \frac{N}{A_i} \\ \sigma_s &= \alpha_e \sigma_c \end{aligned}$$

Assuming the characteristic value of the force, these formulas are therefore used for serviceability verifications such as $\sigma_c < \bar{\sigma}_c$ (with $\bar{\sigma}_c = 0.45 f_{ck}$ for non-transient load situations).

For *resistance verification* (at the ultimate limit state) the assumption of elasticity should be replaced by the constitutive models σ - ε of the two materials (see Fig. 2.5). In addition to what mentioned in Sect. 1.4.2 about concrete models, it is to be noted that the ultimate strain ε_{cu} is reached under an imposed contractions. If

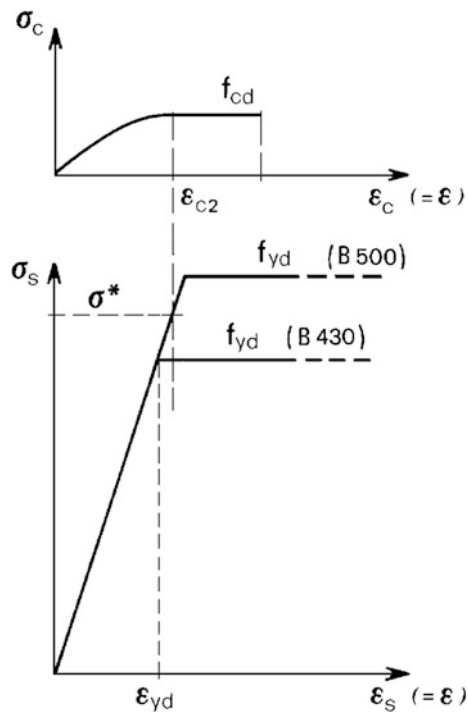
otherwise it is the load that increases, rupture occurs at the value ε_{c1} (see Fig. 1.4) suddenly developing with the uncontrolled failure of the specimen.

In concrete sections in bending, the variability of stresses provides a certain degree of redundancy to the system and therefore the less stressed fibres offer a control to the deformation of the more stressed ones. The beam edges in compression can therefore reach the limit ε_{cu} . On the contrary in concrete sections under axial compression there is no degree of redundancy, as all fibres are equally stressed. For this reason, the limit ε_{c1} shall be assumed as ultimate failure contraction.

The presence of steel reinforcement, if not already yielded, could provide in RC sections the deformations control to pass the limit ε_{c1} . This is valid up to the yield point of the reinforcement itself, at which any internal redundancy is lost. The problem does not have any practical relevance, as the viscous strain increment is to be added to the limit $\varepsilon_{c2} \cong \varepsilon_{c1} \cong 0.002$ and this always leads steel to yield, as it will be shown hereafter.

In the analysis of a section at the ultimate limit state, as indicated in Fig. 2.5, the parabola-rectangle model is assumed for concrete, where the ultimate failure contraction is approximated by the value ε_{c2} ; moreover, the elastic-perfectly plastic model is assumed for steel, disregarding hardening which is negligible at the failure limit ε_{c2} of the section anyway.

Fig. 2.5 Stress-strain diagrams of concrete and steel



Assuming for now an instantaneous load increment, at the mentioned failure limit ε_{c2} of the most brittle material, the equilibrium of the section is therefore set with the equation:

$$N_{Rd} = f_{cd}A_c + \sigma^* A_s$$

where it should be set $\sigma^* = E_s \varepsilon_{c2}$ if $\varepsilon_{yd} > \varepsilon_{c2}$, or $\sigma^* = f_{yd}$ if $\varepsilon_{yd} < \varepsilon_{c2}$.

Similarly to the elastic formula, this equation, for $\sigma^* = f_{yd}$, can be set as

$$N_{Rd} = f_{cd} \left(A_c + \frac{f_{yd}}{f_{cd}} A_s \right) = f_{cd} A_{ir}$$

where *the ideal area equalized to concrete is*

$$A_{ir} = A_c + \frac{f_{yd}}{f_{cd}} A_s = A_c (1 + \omega_s)$$

The homogenization coefficient of the steel area is here given by the ratio of the two strength values, whilst the dimensionless coefficient

$$\bar{\omega}_s = \frac{f_{yd} A_s}{f_{cd} A_c}$$

where the areas of the two materials are weighed with the respective strengths, is called *mechanical reinforcement ratio*. It indicates the relative contribution of the steel reinforcement to resistance.

In order to give the order of magnitude of such contribution, three situations are hereafter evaluated: a lower one corresponding to the minimum limit of 0.3% of geometric reinforcement ratio and to the association of steel B450C with the highest class of concrete; an upper one corresponding to the maximum limit of 4% of steel reinforcement ratio and the association of steel B450C with the lowest class of concrete; an intermediate one corresponding to a geometrical percentage of 0.8% and to a more balanced association of materials. Assuming, therefore $\gamma_s = 1.15$, $\gamma_c = 1.50$ and $\alpha_{cc} = 0.85$ one has:

$$\omega_s = 0.003 \frac{450/1.15}{0.85 \times 70/1.50} \cong 0.03$$

$$\omega_s = 0.040 \frac{450/1.15}{0.85 \times 16/1.50} \cong 1.73$$

$$\omega_s = 0.008 \frac{450/1.15}{0.85 \times 30/1.50} \cong 0.21$$

It is noted how it is possible to go from low reinforcement elements with steel contribution practically negligible to situations, not frequent in reality, where the

reinforcement contribution is predominant. In common situations, the presence of reinforcement can increase the load capacity of columns approximately by 20% or 30%, this being on average the mechanical reinforcement percentage.

It is eventually to be noted that several design codes impose to take into account a minimum eccentricity of the axial force, for example with $e \geq 0.05 h$, where h is the depth of the section. The verification therefore refers to combined action of axial force and bending moment (see Chap. 6). Moreover, for moderate reinforcement ratios (approximately $\omega_s \leq 0.8$), such requirement remains implicitly fulfilled if, in the formula of verification of centred axial force, the concrete contribution is penalized attributing with $0.8f_{cd}$. In such case, fixing the value of mechanical reinforcement ratio, the formula deduced here becomes

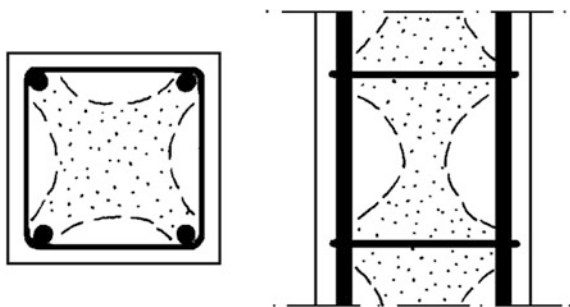
$$N_{Rd} = f_{cd}A_c(0.8 + \omega_s)$$

2.1.2 Effect of Confining Reinforcement

The external cage made of stirrups and longitudinal bars provides a certain degree of confinement of concrete inside the column, counteracting the transverse expansion under loads and increasing the resistance. The effect in ordinary columns with stirrups is moderate because of the low density of the steel reinforcement mesh. As indicatively shown in Fig. 2.6, the low flexural stiffness of the straight portions of bars leaves the confining actions concentrated on the bends of the stirrups; such actions then diffuse on a limited internal portion of concrete.

In order to systematically take advantage of the effect described above, appropriate reinforcing hoops are adopted, much more closely spaced than in ordinary columns with stirrups. The *confined columns* therefore have a number of longitudinal bars (at least 6), closely distributed on a circular external perimeter and enclosed by a spiral bar (or circular links). The pitch of the spiral has to be properly limited with respect to the diameter, for example with $s \leq D/5$. In this way, an effective confinement of transverse expansions is obtained in the entire concrete cylindrical core delimited by the hoops (see Fig. 2.7).

Fig. 2.6 Confining action on the concrete core



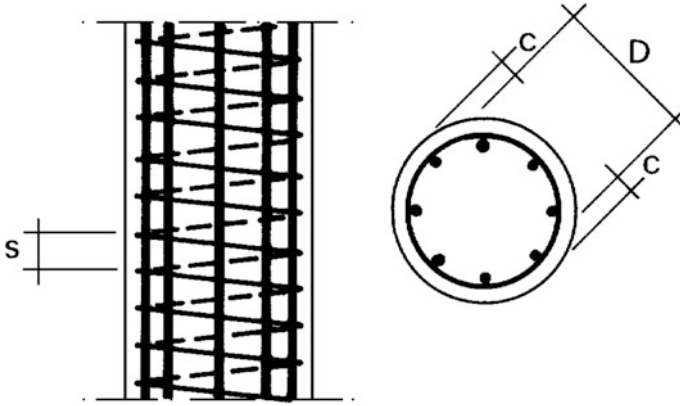


Fig. 2.7 Details of a confined column

In the elastic range, the effect of confinement on the stress distribution is very low, as shown hereafter.

Having defined $A_n = \pi D^2/4$ as the area of the core, A_l the area of the longitudinal reinforcement and $A_w = a_w \pi D/s$ the equivalent one of the spiral bar (of cross section a_w), the following relations are obtained. The isolated segment of the core of height s , subject to a vertical flux of stresses σ_v (see Fig. 2.8a) exhibits a shortening

$$\delta_{vo} = \frac{\sigma_v}{E_c} s$$

and, at the same time, an horizontal expansion

$$\delta_{ho} = -\nu \frac{\sigma_v}{E_c} D$$

The hoops oppose to such expansion with a horizontal stress σ_h (see Fig. 2.8b, c) which can be considered as the unknown of the problem. For the equilibrium of the semicircular piece of bar of Fig. 2.8c also the stress σ_w in the spiral can be expressed in terms of σ_h :

$$2 \sigma_w a_w = \sigma_h D s$$

whence

$$\sigma_w = \frac{Ds}{2a_w} \sigma_h = \frac{A_n}{\pi D^2/4} \frac{Ds}{2a_w} \sigma_h = 2 \frac{A_n}{A_w} \sigma_h$$

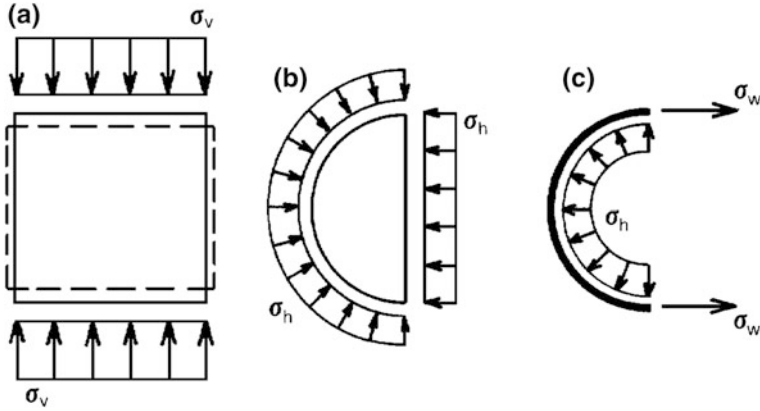


Fig. 2.8 Equilibrium conditions of concrete core and confining steel

The relative horizontal expansion between spiral and core due to the unknown σ_h is therefore obtained adding up the two deformation contributions of steel and concrete:

$$\delta_{hh}\sigma_h = D \left\{ \frac{\sigma_w}{E_s} + \frac{1-\nu}{E_c} \sigma_h \right\} = D \left\{ \frac{2A_n}{E_s A_w} + \frac{1-\nu}{E_c} \right\} \sigma_h$$

Eventually the compatibility of deformations is set between spiral and core:

$$\delta_{hh}\sigma_h + \delta_{ho} = 0$$

from which one obtains

$$\sigma_h = -\frac{\delta_{ho}}{\delta_{hh}} = \frac{\frac{\nu}{E_c}}{\frac{2A_n}{E_s A_w} + \frac{1-\nu}{E_c}} \sigma_v$$

that, with $\rho_w = A_w/A_n$, $\alpha_e = E_s/E_c$ and $\psi_w = \alpha_e \rho_w$, becomes:

$$\sigma_h = \frac{1}{\frac{2}{\psi_w} + \frac{1}{1-\nu} + 1} \frac{\nu}{1-\nu} \sigma_v$$

Without the spiral ($\psi_w = 0$) one has $\sigma_h \equiv 0$: it is the case of ordinary columns with stirrups. The maximum confining contribution is obtained instead at the limit situation of a spiral of so high size that it can be considered rigid with respect to concrete ($\psi_w = \infty$).

In this case one obtains

$$\sigma_h = \frac{v}{1-v} \sigma_v$$

$$(\sigma_h \cong 0.25 \sigma_v \quad \text{for} \quad v \cong 0.20)$$

The vertical contraction of the confined column is therefore:

$$\varepsilon_v = \frac{1}{E_c} (\sigma_v - 2v\sigma_h) = \frac{\sigma_v}{E_c} \left(1 - \frac{2v^2}{1-v} \right)$$

less than the one of the ordinary column, as if concrete had an effective elastic modulus

$$E'_c = \frac{E_c}{1 - \frac{2v^2}{1-v}} = \frac{1-v}{(1+v)(1-2v)} E_c$$

With this effective elastic modulus, increased by about 10% with respect to the ordinary one as it can be deduced setting $v \cong 0.20$, the *elastic design* can be carried evaluating the stresses on the plane section of the column for a given axial force:

$$N = A_n \sigma_v + A_1 \sigma_1 = \sigma_v (A_n + \alpha'_e A_1) = \sigma_v A'_i$$

being, with $\alpha'_e = E_s/E'_c \cong 0.9\alpha_e$ and with, $\psi'_1 = \alpha'_e \rho_1$,

$$A'_i = A_n (1 + \psi'_1)$$

the equivalent area. For longitudinal bars of about 1% with respect to the cross section of the core, with $6 \leq \alpha_e \leq 10$, values increased by about 1% are obtained for the stress σ_v in concrete, values decreased by about 9% are obtained for stress σ_1 in the longitudinal reinforcement.

Considering that the actual elastic deformability of the spiral further reduces this effect, which remains still limited to the concrete core excluding the external cover layer of thickness c , it can be seen how, in the elastic design, it can be neglected.

The *ultimate resistance* is instead significantly increased by the confinement as indicated in the following formulation which is based on the experimental results. First of all, the tests on confined columns exhibit early spalling outside the confining hoops. This occurs at level of the stresses close to the uniaxial strength f_c of concrete.

As the load N further increases, more significant transversal expansions of the core are observed, greatly increasing close to the ultimate limit, inducing tensions in the spiral reinforcement. If abnormal quantities of this reinforcement are excluded, the column failure occurs after the spiral yields. Failure itself, by crushing of the

concrete core, is characterized by high values of the contraction ε_v to which also corresponds the yielding of the longitudinal reinforcement. The stresses σ_{vr} of the concrete core measured at ultimate limit state are much higher than the uniaxial strength f_c . The increase in strength appears to depend linearly on the confining stress σ_{hr} given by the spiral:

$$\sigma_{vr} = f_c + \kappa \sigma_{hr}$$

Actually the different tests lead to significantly discordant values of κ : an estimate precise and reliable enough for such coefficient is still not available, with the consequence of the need to penalize the resisting effect of spirals with greater factors of safety.

Integrating therefore the assumptions with what results from the findings mentioned above, the equilibrium of the section at the ultimate limit state is:

$$N_r = A_n(f_{cd} + \kappa\sigma_{hr}) + A_l\sigma_{lr}$$

where the first term represents the contribution of the concrete core, the second one represents the contribution of the longitudinal reinforcement.

Since

$$\sigma_h = \frac{1}{2} \frac{A_w}{A_n} \sigma_w$$

setting $\sigma_{wr} = \sigma_{lr} = f_y$ and introducing the design values of the semi-probabilistic method, one eventually obtains

$$N_{Rd} = f_{cd} \left(A_n + \frac{f_{yd}}{f_{cd}} A_l + \frac{\kappa f_{yd}}{2 f_{cd}} A_w \right) = f_{cd} A'_{ir}$$

where the homogenization coefficients of the two types of reinforcement (longitudinal and transverse) are distinguished by the factor $\kappa/2$. Assuming for example $\kappa = 4$ (see formula $\bar{\sigma}_1 = 1 + \bar{\sigma}_2$ of Sect. 1.1.3 for triaxial stress states with $\bar{\sigma}_1 \gg \bar{\sigma}_2 = \bar{\sigma}_3$), one obtains

$$N_{Rd} = f_{cd} A_n (1 + \omega_l + 2\omega_w)$$

where it can be noted that, in terms of resistance contribution, the mechanical ratio $\omega_w = f_{sd} A_w / f_{cd} A_n$ of the confining reinforcement is weighed twice as much as the one of the longitudinal reinforcement. However, there is a limit $A_w \leq 2A_l$ for the confining reinforcement with respect to the longitudinal one, beyond which a failure by transverse shearing of the column occurs at lower load levels than the one deducible from the equation set above. The usual limitation to the longitudinal reinforcement ratio is to be eventually added, related to bond problems. Such limitation for confined columns can be set as $A'_{ir} \leq 2A_n$.

The comparison with the capacity of ordinary columns with stirrups can be deduced equating the contribution of reinforcement in the two cases:

$$\omega_1 = \omega_1 + 2 \omega_w$$

which leads, for the same materials, to the relationship $A_s = (5/3)A_t$, having set $A_w = 2A_t$, having indicated with $A_t = A_1 + A_w$ the total reinforcement of the confined column and with A_s the longitudinal reinforcement of the ordinary columns. Taking into account the additional presence of the stirrups, one can deduce that the circular arrangement allows to roughly halve the amount of reinforcement for the same capacity and the same size of concrete. This does not contemplate possible problems of shape, which is limited to the circle or the equilateral polygon for confined sections, nor economical problems which normally lead to prefer, where permitted, an increase in the area of concrete instead of the confining reinforcement.

In order to take into account a minimum load eccentricity, introducing for the confined columns the same reduction in concrete resistance as for the ordinary columns, one eventually obtains the (conservative) formula of the design resistance

$$N_{Rd} = f_{cd} A_n (0.8 + \omega_1 + 1.6\omega_w)$$

which reevaluates the contribution of longitudinal reinforcement with respect to concrete and its confining reinforcement.

2.1.3 Effects of Viscous Deformations

The formulas of elastic design presented before give the stresses for a short-term loading. Starting from these initial values, the permanence of loads leads to a slow redistribution of stresses between concrete and steel as a result of creep.

For an axial force N constant in time, the equilibrium of the section of Fig. 2.4 leads to equate the force increment that occurs in steel between time t and time $t + dt$ to the decrement that simultaneously occurs in concrete:

$$A_s d\sigma_s(t) = -A_c d\sigma_c(t)$$

The compatibility formulated in the same time interval leads to equate the strain increments $d\varepsilon_s$ and $d\varepsilon_c$ of steel and concrete. The first one derives from the law of elasticity, the second one from the law of linear creep with variable stresses:

$$\varepsilon(t) = \frac{1}{E_c} \left\{ \sigma(t) + \int_{t_0}^t \sigma(\tau) \Phi(t, \tau) d\tau \right\}$$

where it is reminded that the creep kernel

$$\Phi(t, \tau) = -\frac{\partial \varphi(t, \tau)}{\partial \tau}$$

gives the elementary contribution of a load pulse $\sigma(\tau)d\tau$ applied at the intermediate time τ (see Fig. 1.18b). If, for concrete loaded at an early age, an ageing model is assumed with:

$$\varphi(t, \tau) = c(t) - c(\tau)$$

one therefore obtains that each load pulse produces creep effects only within the interval of application contiguous to τ . These effects remain then unchanged:

$$\Phi(t, \tau) = -\frac{\partial \varphi(t, \tau)}{\partial \tau} = \Phi(\tau) = \left[\frac{\partial \varphi(t, \tau)}{\partial \tau} \right]_{t=\tau}$$

From the fundamental theorem of calculus one obtains in this case

$$\frac{d}{dt} \int_{t_0}^t \sigma(\tau) \Phi(\tau) d\tau = \sigma(t) \Phi(t) = \sigma(t) \frac{d\varphi(t)}{dt}$$

which allows to eventually write the compatibility equation as

$$\frac{d\sigma_s(t)}{E_s} = \frac{d\sigma_c(t)}{E_c} + \frac{\sigma_c(t)}{E_c} d\varphi(t)$$

Replacing now in this equation the value $d\sigma_s = -d\sigma_c/\rho_s$ derived from the equilibrium, one has (with $\alpha_e = E_s/E_c$ and $\psi_s = \alpha_e \rho_s$):

$$-\left(1 + \frac{1}{\psi_s}\right) d\sigma_c = \sigma_c d\varphi$$

Setting for brevity

$$\beta = \frac{\psi_s}{1 + \psi_s}$$

one obtains the differential equation

$$\frac{d\sigma_c}{\sigma_c} = -\beta d\varphi$$

with separation of variables which, integrated between t_0 and t , leads to:

$$\ln \sigma_c(t) - \ln \sigma_{c0} = -\beta \varphi(t)$$

with $\sigma_{c0} = \sigma_c(t_0)$ and $\varphi(t_0) = 0$. Stresses in concrete therefore decrease, starting from an initial value

$$\sigma_{c0} = \frac{N}{A_c + \alpha_e A_s} = \frac{N}{A_c(1 + \psi_s)}$$

with an exponential rate:

$$\sigma_c(t) = \sigma_{c0} e^{-\beta \varphi(t)}$$

down to stabilization on the final value

$$\sigma_{c\infty} = \sigma_{c0} e^{-\beta \varphi_\infty}$$

to which for equilibrium corresponds in steel the stress

$$\sigma_{s\infty} = \frac{N - A_c \sigma_{c\infty}}{A_s} = \frac{1 + \psi_s - e^{-\beta \varphi_\infty}}{\rho_s} \sigma_{c0}$$

The ratio between stresses in the two materials becomes:

$$\alpha_e^* = \frac{\sigma_{s\infty}}{\sigma_{c\infty}} = \alpha_e \frac{1 + \psi_s - e^{-\beta \varphi_\infty}}{\psi_s - e^{-\beta \varphi_\infty}} = \alpha_e \left(\frac{e^{\beta \varphi_\infty}}{\beta} - \frac{1}{\psi_s} \right)$$

which allows to apply under viscoelastic conditions the same formulas of the elastic design where the *modified coefficient* α_e^* is to be introduced for the homogenization of steel areas, properly increased with respect to the elastic short-term one α_e . A *viscoelastic reinforcement ratio* can therefore be defined

$$\psi_s^* = \alpha_e^* \rho_s$$

with which one can estimate the final stresses

$$\begin{aligned} \sigma_{c\infty} &= \frac{N}{A_c(1 + \psi_s^*)} \\ \sigma_{s\infty} &= \alpha_e^* \sigma_{c\infty} \end{aligned}$$

In order to show the order of magnitude of creep effects in a reinforced concrete column, let us consider a section with $\rho_s = 0.008$, $\alpha_e = 6$ and $\varphi_\infty = 2.4$.

With these values one can deduce (with $\psi_s = 0.048$ and $\beta = 0.0458$):

$$\begin{aligned}\alpha_e^* &= \left(\frac{e^{\beta\varphi_\infty}}{\beta} - \frac{1}{\psi_s} \right) \alpha_e = 3.54\alpha_e \\ \psi_e^* &= \alpha_e^* \rho_s = 0.170 \\ \sigma_{c\infty} &= \frac{1 + \psi_s}{1 + \psi_s^*} \sigma_{co} = 0.896\sigma_{co} \\ \sigma_{s\infty} &= \frac{\alpha_e^* \sigma_{c\infty}}{\alpha_e^* \sigma_{co}} \sigma_{so} \cong 3.17\sigma_{so} \\ \varepsilon_\infty &= \frac{\sigma_\infty}{\sigma_{so}} \varepsilon_0 \cong 3.17\varepsilon_0\end{aligned}$$

It can be noted how, further to a limited reduction of stresses in concrete, stresses in steel can increase more than three times. Further significant increases are caused by the shrinkage as analysed in Sect. 2.2.1.

If one assumed the approximate technical method (see Sect. 1.3.3), evaluating creep effects on the basis of the initial stress in concrete, one would have:

$$\begin{aligned}\Delta\varepsilon &= \frac{\sigma_{co}}{E_c} \varphi_\infty = 2.40\varepsilon_0 \\ \Delta\sigma_s &= E_s \Delta\varepsilon = \alpha_e \sigma_{co} \phi_\infty = 2.40\sigma_{so} \\ \Delta\sigma_c &= -\rho_s \Delta\sigma_s = -\psi_s \sigma_{co} \phi_\infty = 0.115\sigma_{co} \\ \sigma_{c\infty} &= \sigma_{co} - \Delta\sigma_c = 0.885\sigma_{co} \\ \sigma_{s\infty} &= \sigma_{so} - \Delta\sigma_s = 3.40\sigma_{so} \\ \varepsilon_\infty &= \varepsilon_0 - \Delta\varepsilon = 3.40\varepsilon_0\end{aligned}$$

with the overestimation of the effects.

Instead, if one assumed the effective modulus method (EMM of Sect. 1.3.3), evaluating the creep effects on the basis of the final stress in concrete, one would have:

$$\begin{aligned}E_c^* &= \frac{E_c}{1 + \phi} = \frac{E_c}{3.40} \\ \alpha_e^* &= E_s / E_c^* = 3.40\alpha_e \\ \psi_s^* &= \alpha_e \rho_s = 0.163 \\ \sigma_{c\infty} &= \frac{1 + \psi_s}{1 + \psi_s^*} \sigma_{co} = 0.901\sigma_{co} \\ \sigma_{s\infty} &= 3.40 \times 0.90 \sigma_{so} = 3.06 \sigma_{so} \\ \varepsilon_\infty &= 3.06 \varepsilon_0\end{aligned}$$

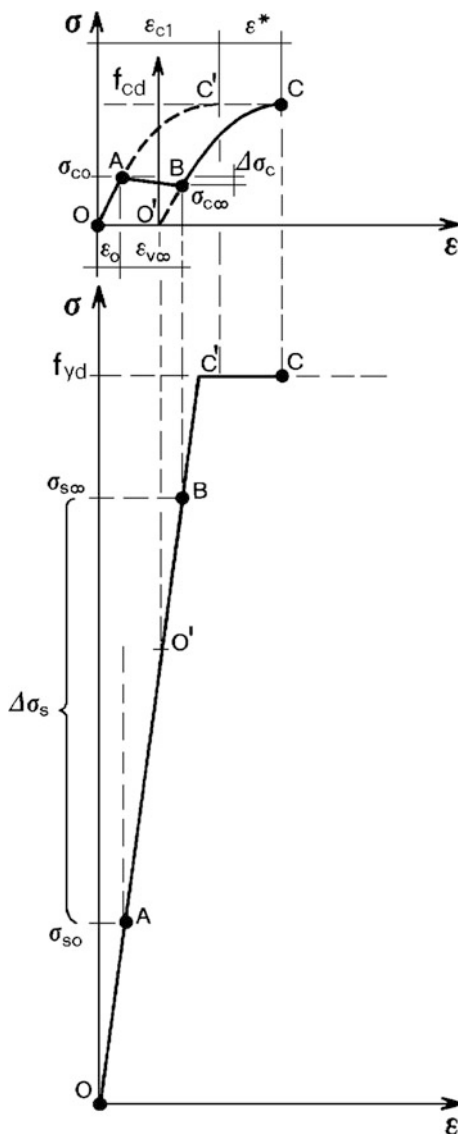
with the underestimation of the effects.

Effects on Strength

In order to evaluate the creep effects on the ultimate strength, the load history should be followed considering first the application of permanent actions, then the development of the consequent creep deformations with relative redistributions of stresses and eventually the final increase of variable loads up to failure. The conventional procedure starts from the characteristic values of permanent loads.

The σ - ε diagrams of the materials of Fig. 2.9 show an initial short-term segment O - A essentially linear also for concrete. The slow rearrangement of the section

Fig. 2.9 Creep effects on stress-strain diagrams



follows (segment $A-B$) which shifts by $\varepsilon_{v\infty}$ in obedience to the laws of equilibrium and viscoelastic compatibility developed above.

The creep process led at its end to an increase $\Delta\sigma_s$ of the stress in steel and to a complementary relaxation $\Delta\sigma_c$ of the stress in concrete. Then a new instantaneous load follows the shifted σ_c - ε curve shown in the Fig. 2.9.

For example, in order to decompress concrete (segment $B-O'$) an expansion $\sigma_{c\infty}/E_c$ ($<\varepsilon_o$) would be necessary. At the same time steel would unload by $\alpha_e\sigma_{c\infty}$. At the new origin O' a residual stress $\sigma_{s\infty}-\alpha_e\sigma_{c\infty}$ would therefore remain in the reinforcement. The unloading of the external actions would lead to self-stresses $\sigma_c = \sigma_c$ in tension in concrete and $\sigma_s = \Delta\sigma_s = -\Delta\sigma_c/\rho_s$ in compression in steel, with a residual contraction of the column equal to $\Delta\sigma_s/E_s$.

If the load is increased from B up to failure, the point C of the shifted curve is reached, with a contraction greater by $\varepsilon^* = \varepsilon_{v\infty} - \Delta\sigma_c/E_c$ with respect to the contraction ε_{c1} of a short-time loading.

With respect to the model for the resistance verification of the section under short-term loading, valid for the initial stages, the one at t_∞ requires the simple translation of the diagram σ_c - ε by a segment

$$\varepsilon^* = \varepsilon_{v\infty} - \frac{\Delta\sigma_c}{E_c} = \frac{\Delta\sigma_s}{E_s} \left(1 - \alpha_e \frac{\Delta\sigma_c}{\Delta\sigma_s} \right) = \frac{\Delta\sigma_s}{E_s} (1 + \psi_s)$$

The ultimate resistance basically does not change since the stress $\sigma_s = f_{yd}$ in steel remains constant from C' to C :

$$N_{Rd} = A_c f_{cd} + A_s f_{yd}$$

In the case of high-strength steel for which $\varepsilon_{c1} < \varepsilon_{yd}$, the accumulation $\varepsilon_{c1} + \varepsilon^*$ of the contractions at failure leads to a delayed yield of reinforcement and to a final resistance capacity that is given again by the formula shown above.

2.2 Tension Elements

With the section on reinforced concrete tie elements, the fundamental topic of cracking is introduced, which will be analysed again and developed hereafter with reference to elements in bending. The topic is very broad, involving static, chemical and technological aspects, and good levels of accuracy in the relative applicative calculations have not currently been achieved. Criteria and methods remain still open to considerable refinements.

Further to the analyses of the cracking process, the topic of prestressing is introduced, considered as measure to keep cracking within appropriate service limits. On one hand therefore the possibility to satisfy, even for elements in tension, specific functional requirements; on the other hand the possibility of the full use of the resources of high-strength steel, as it will be better clarified hereafter.

Taken for granted the safety with respect to collapse, cracking has nevertheless three orders of consequences:

- the *loss of tightness*, generally not relevant, in some cases related to functional requirements (such as waterproofing of tanks), in other cases seriously detrimental with respect to durability (such as freeze/thaw phenomena that can progressively disintegrate concrete if exposed in climates with strong daily temperature ranges around zero);
- the *aesthetic decay* associated to the possible evidence of the cracking pattern and the sense of apparent static deficiency which make it unacceptable to users;
- the *damage of protection* against corrosion of the reinforcement, provided by the appropriate concrete cover, with uncertain durability of the resistance.

2.2.1 Verifications of Sections

If one assumes that concrete resists in tension, deforming elastically with a modulus E_{ct} , the calculation of stresses in the section of a RC tie subject to an axial tension force N leads to the same formula deduced for columns. With the usual assumptions related to the uncracked section, equilibrium leads to

$$\sigma_c = \frac{N}{A_c + \alpha_{et}A_s} \quad \sigma_s = \alpha_{et}\sigma_c$$

where $\alpha_{et} = E_s/E_{ct}$ is the coefficient of homogenization of the reinforcement area.

Such formulas are used for *serviceability verifications* that do not concern the ultimate capacity of the structure. In particular with those formulas, given $\sigma_c = f_{ctk}$, the limit of cracks formation is defined, according to what is specified later on. With respect to collapse instead, the tensile strength of concrete is not proven to be reliable enough. Certain phenomena, commonly neglected in the normal resistance calculations, can in fact contribute to early cracking, to a degree which is often difficult to estimate.

Effects of Shrinkage

Tensile stresses occur in concrete, even before that the structure is subject to service loads, because of shrinkage. For the cross section of an element in RC, such effect can be estimated imposing equilibrium and compatibility at time t to which the value $\varepsilon_{CS}(t)$ of shrinkage corresponds, related to concrete only:

$$A_s\sigma_s(t) + A_c\sigma_c(t) = 0$$

$$\frac{\sigma_s(t)}{E_s} = \frac{\sigma_c(t)}{E_{ct}} + \varepsilon_{cs}(t)$$

From the first equation one obtains:

$$\sigma_s(t) = -\frac{1}{\rho_s} \sigma_c(t)$$

which, substituted in the second one, leads to

$$\sigma_c(t) = -\beta E_{ct} \varepsilon_{CS}(t)$$

where

$$\beta = \frac{\psi_{st}}{1 + \psi_{st}}$$

with $\psi_{st} = \alpha_{et} \rho_s$.

Assuming for the contraction $\varepsilon_{cs}(t)$ the absolute value, the negative sign of the formula indicates a tensile stress $\sigma_c(t)$.

In order to give a qualitative indication about this phenomenon, one can consider the same cross section analysed at Sect. 2.1.3 with respect to the creep effects in the columns. Given that the limited level of tensile stresses allows to assume an elastic modulus $E_{ct} = E_c$, with $\rho_s = 0.008$ and $\alpha_{et} = 6$ ($E_c \cong 34,000$ N/mm²), for a final value of shrinkage $\varepsilon_{cs\infty} = 0.00036$ one has (with $\psi_{st} = 0.048$ and $\beta = 0.0458$):

$$\sigma_{c\infty} = -0.56 \text{ N/mm}^2 \quad (\text{tension})$$

$$\sigma_{s\infty} = +70.1 \text{ N/mm}^2 \quad (\text{compression})$$

High reinforcement ratios increase tensile stresses in concrete, reducing compressions in steel to a lesser extent. Creep mitigates the phenomenon with time, same as for the common permanent actions. Neglecting the effects of simultaneous interaction between the two phenomena, the self-induced stresses due to shrinkage can be interpreted as instantaneous initial values followed by the slow viscous relaxation of stresses. This can be evaluated using the criteria defined in Sect. 2.1.3.

For the same cross section analysed above, following the criterion of the effective Modulus which underestimates the reduction of self-induced stresses, with $\varphi_\infty = 2.4$, for example one would therefore have:

$$E_{ct}^* = E_{ct}/(1 + \varphi_\infty) = E_{ct}/3.40; \quad \alpha_{et}^* = E_s/E_{ct}^* = 3.4\alpha_{et}$$

$$\psi_{st}^* = \alpha_{et}^* \rho_s = 3.4\psi_{st};$$

$$\beta^* = \psi_{st}^*/(1 + \psi_{st}^*) = 0.1403$$

$$\sigma'_{c\infty} = -\beta^* E_{ct}^* \varepsilon_{cs\infty} = -0.90 \sigma_{c\infty}$$

$$\sigma'_{s\infty} = -\sigma'_{ct}/\rho_s = 0.90 \sigma_{s\infty}$$

with a reduction of 10% of the effects with respect to the initial values.

Cracked Section

Therefore in the RC ties, the self-induced stresses due to shrinkage, added to stresses due to external loads, induce early concrete cracks. If now the assumption of cracked sections with $f_{ct} = 0$ is made, the resisting part of the tie is limited to the only reinforcement steel. The calculation is simply reduced to

$$\sigma_S = \frac{N}{A_S}$$

and, at the ultimate limit state, according to the elastic-perfectly plastic model, the capacity is given by

$$N_{Rd} = f_{yd} A_S$$

whilst according to the bilinear model with hardening, the capacity is given by

$$N_{Rd} = f'_{td} A_S$$

These formulas verify safety to failure of the tie; they do not give any indication about the cracking pattern under service loads. And the cracking verification, according to criteria shown hereafter, could give more restrictive limits to the design of the tie member.

2.2.2 Prestressed Tie Members

If cracking in service is to be avoided or limited, prestressing has to be applied to the tie. Naming σ_p the stress in the special cable centred in the section, pretensioned at a value ε_{po} of the strain before being locked with concrete, and with σ_s the stress in the ordinary passive reinforcement, the elastic compatibility of the section is imposed as:

$$\frac{\sigma_c}{E_c} = \frac{\sigma_S}{E_S} = \frac{\sigma_p}{E_p} - \varepsilon_{po}$$

from which one has

$$\begin{aligned}\sigma_S &= \alpha_e \sigma_c \\ \sigma_p &= \alpha_e \sigma_c + \sigma_{po}\end{aligned}$$

having indicated with $\sigma_{po} = E_S \varepsilon_{po}$ the pretension in the cable at concrete decompression ($\sigma_c = 0$).

For the equilibrium of the section subject to an axial force N coming from external loads, with obvious meaning of the symbols one has:

$$N = \sigma_c A_c + \sigma_s A_s + \sigma_p A_p$$

from which by substitution one obtains:

$$N = \sigma_c (A_c + \alpha_e A_s + \alpha_e A_p) + N_{po}$$

with

$$N_{po} = \sigma_{po} A_p$$

prestressing force in the tie.

For the *verification of stresses* in service one therefore obtains:

$$\sigma_c = \frac{N}{A_i} - \frac{N_{po}}{A_i}$$

which shows the positive contribution of prestressing in controlling tensile stresses in concrete, being able to fulfil, for ties also, the limit $\sigma_c \leq 0$ which leads to $N \leq N_{po}$.

The equivalent area of the section equalized to concrete is given by

$$A_i = A_c (1 + \alpha_e \rho_s + \alpha_e \rho_p) = A_c (1 + \alpha_e \rho_t) = A_c (1 + \psi_t)$$

where the total area of reinforcement $A_t = A_s + A_p$ is equalized with the usual coefficient of homogenization $\alpha_e = E_s/E_c$, whilst in relative terms the increasing contribution is expressed in terms of the reinforcement elastic ratio $\psi_t = \alpha_e \rho_t = \psi_s + \psi_p$.

Imposing $N = 0$, the self-induced stresses due to prestressing, corresponding to the absence of external loads, are obtained as:

$$\sigma_c = -\frac{N_{po}}{A_i}; \quad \sigma_s = -\alpha_e \frac{N_{po}}{A_i}; \quad \sigma_p = \sigma_{po} - \alpha_e \frac{N_{po}}{A_i}$$

showing compressive stresses in concrete and passive reinforcement, tensile stresses in the pretensioned reinforcement. This situation is indicated by the dots in the diagrams of Fig. 2.10.

Under the assumption of *cracked section*, for $\sigma_c > 0$ (in tension), the equilibrium with the external force N is to be related to the steel part only of the section, both passive and pretensioned:

$$\sigma_s = \frac{N}{A_t} - \frac{N_{po}}{A_t}$$

$$\sigma_p = \frac{N}{A_t} + \beta \frac{N_{po}}{A_t}$$

with $\beta = A_s/A_p$. If the elastic-perfectly plastic σ - ε model is adopted for both reinforcements, passive and pretensioned, the *ultimate resistance* in tension is defined by a value of the elongation to which the yielding of both reinforcements corresponds. In this case one therefore obtains

$$N_{Rd} = f_{yd}A_s + f_{yd}A_p$$

formula that does not depend on the initial stress σ_{po} in the cable. Prestressing therefore does not affect the ultimate capacity of the tie, whereas it has significant effects on the serviceability states where there is still an elastic behaviour of the materials.

Adopting the bilinear model with hardening, failure of the tie in tension is determined by the ultimate strain ε_{pud} of prestressing steel, which is the less ductile and was already subject pretensioning ε_{po} before being locked with concrete. At this ultimate limit, the passive steel has reached the strain

$$\varepsilon_s = \varepsilon_{pud} - \varepsilon_{po} < \varepsilon_{ud}$$

The ultimate capacity therefore becomes

$$N_{Rd} = \sigma_s A_s + f'_{ptd} A_p$$

with $\sigma_s = \sigma_s(\varepsilon_s)$. Having for common materials $\varepsilon_s > \varepsilon_{yd}$, one has

$$\sigma_s = f_{yd} + E_1(\varepsilon_s - \varepsilon_{yd})$$

In this case, prestressing ε_{po} affects directly the resistance of the tie by the reduction of the strain ε_s of passive reinforcement and therefore of its contribution to the rupture limit. The effect is small and, once again, prestressing remains determining for serviceability limit states.

Other than limiting tensile stresses in concrete and affecting the cracking pattern, prestressing affects the *stress ranges* under variable loads. In fact, if the prestressed tie is designed to remain uncracked (with $\sigma_c < f_{ctk}$), a variation ΔN of axial force induces in the reinforcement steel a variation

$$\Delta\sigma_s = \Delta\sigma_p = \alpha_e \frac{\Delta N}{A_i}$$

significantly lower than the one that would occur in the cracked section, where one would have

$$\Delta\sigma_s = \Delta\sigma_p = \frac{\Delta N}{A_t}$$

In relative terms, the range limitation is in the ratio of

$$\frac{\alpha_e A_t}{A_i} = \frac{\psi_t}{1 + \psi_t}$$

Such effect is very important with respect to fatigue resistance of steel in structures subject to repeated loading cycles.

For external *compression* forces the prestressed tie obviously does not work well, as it can be deduced from the diagrams of Fig. 2.10. In service in fact the stresses σ_c in concrete become greater, whereas at ultimate failure limit the pre-stressing reinforcement is barely utilized or even counterproductive, as in the case of stresses σ_p^* that, at the limit strain ε_{c2} of the section, remain in tension.

2.2.3 Cracking in Reinforced Concrete Ties

In order to analyse the origin of the cracking process, let us consider the element of Fig. 2.11, made of concrete with one hypothetical reinforcing bar of diameter ϕ cast-in along its centreline. Let the element be initially completely uncracked and let us start loading it with a tension force N , of low magnitude, applied at the ends of the steel bar.

After the end segments of a length λ necessary for the diffusion of the force from steel to the entire section, a stress state is established in the entire internal segment of the element which can be calculated with the formulas obtained earlier:

$$\sigma_c = \frac{N}{A_c + \alpha_{et} A_s}; \quad \sigma_s = \alpha_{et} \sigma_c$$

which could be integrated with the contribution of shrinkage and creep. As long as the stress σ_c in concrete remains lower than its tensile strength, such stress state remains qualitatively unchanged, as indicated by the diagrams “a” of Fig. 2.11, where in particular it is to be noted how the bond stress τ_b is activated in the segments of incomplete stress diffusion.

Let us now imagine to increase the force N up to values of σ_c very close to the rupture values. At this point, in the internal segment of the element, where there is a complete distribution of stresses on the entire section, a first crack can arise, located where, due to the variability of the characteristic strength parameters, a section

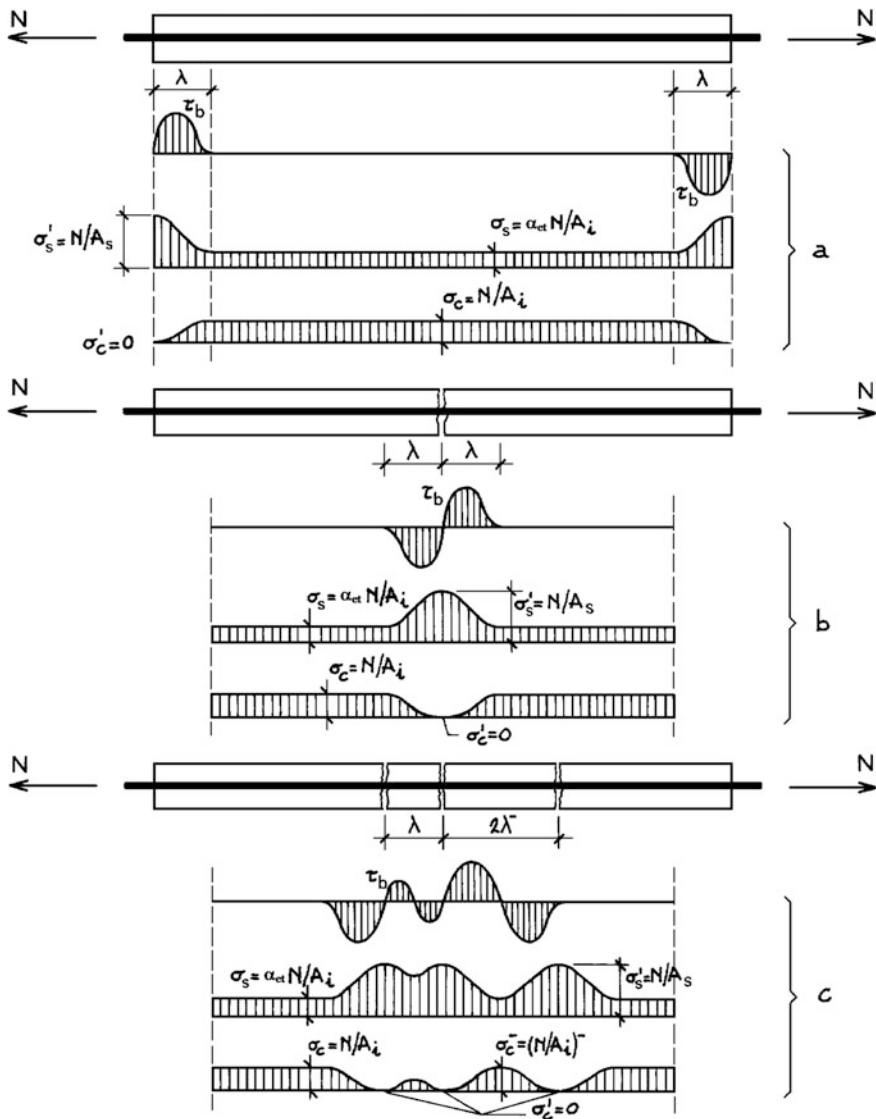


Fig. 2.11 Cracking process in a RC tie

weaker than the others is situated. A new stress state is therefore established, as described by the diagrams “b” of Fig. 2.11, with stresses in the rebar that vary from

$$\sigma'_s = \frac{N}{A_s}$$

at the crack location, to the value σ_s of segments with complete force diffusion, and with stresses in concrete that vary in parallel from 0 to σ_c .

When the force N increases up to overcome the tensile strength of concrete, cracking extends to the entire tie. The minimum distance of a possible subsequent crack from the first one is the parameter λ which characterizes the required length for the complete diffusion of stresses in the section, because only after such length the stress σ_c can reach its maximum value.

The process is qualitatively represented in the diagrams “c” of Fig. 2.11, with the lower and upper limits within which the actual crack spacing s can randomly vary

$$\lambda \leq s < 2\lambda$$

being $s = 2\lambda$ the first value of the distance which allows stress σ_c to reach its maximum value and therefore to introduce a new intermediate crack.

Further increments of N beyond the value of crack formation induce the progressive opening of already existing cracks. Few new cracks can still open in the middle of the longest segments; then the configuration stabilizes with crack widths progressively greater until, for high values of steel strain, bond itself fails.

Crack Spacing

In order to calculate the minimum distance λ between adjacent cracks let us consider the situation of Fig. 2.12 relative to a segment of a tie of length 2λ . Given that the equilibrium of an infinitesimal segment of bar of length dx

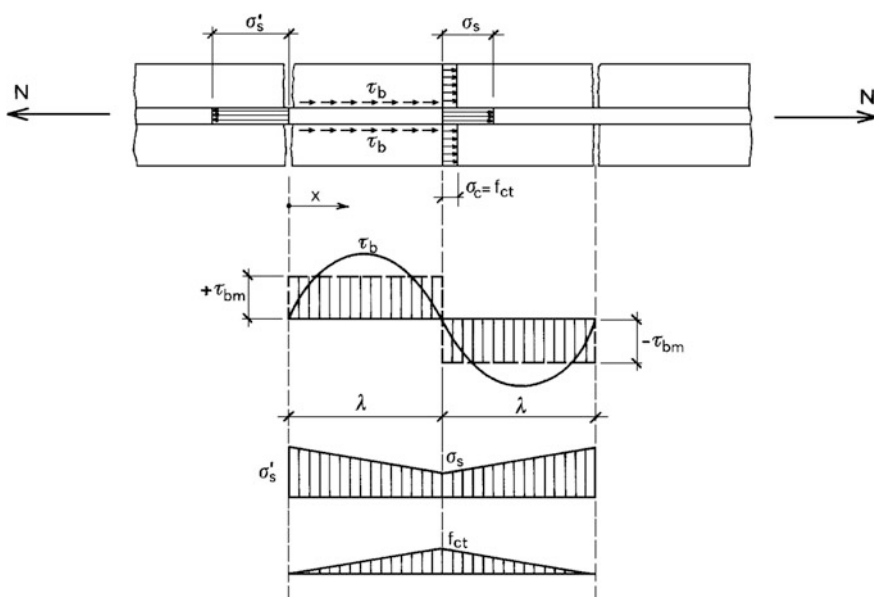


Fig. 2.12 Crack spacing—equilibrium condition

$$A_s d\sigma_s(x) = \pi \phi \tau_b(x) dx$$

leads to express the bond stress in terms of the first derivative of the stress in the steel along the tie:

$$\tau_b(x) = \frac{\phi}{4} \frac{d\sigma_s(x)}{dx}$$

approximating the trend of bond stresses to the constant mean value τ_{bm} , a linear model follows for stresses variations $\sigma_s(x)$ as well as for the complementary stresses in concrete which vary along the centreline following the equilibrium $\sigma_s(x)A_s + \sigma_c(x)A_c \equiv N$. These diagrams are shown in Fig. 2.12, where in particular, at the limit of crack formation, concrete maximum stress is equal to $\sigma_c = f_{ct}$.

For the equilibrium of half segment, one therefore has

$$N = \sigma'_s A_s = \sigma_s A_s + f_{ct} A_c$$

which leads to

$$\Delta\sigma_s = \sigma'_s - \sigma_s = \frac{1}{\rho_s} f_{ct}$$

The equilibrium of half part of the bar is therefore set as

$$A_s \Delta\sigma_s = \int_0^\lambda \pi \phi \tau_b(x) dx$$

which, with the constant model mentioned above, becomes

$$\frac{\pi \phi^2}{4} \Delta\sigma_s = \pi \phi \tau_{bm} \lambda$$

One therefore obtains

$$\lambda = \frac{\phi}{4} \frac{\Delta\sigma_s}{\tau_{bm}} = \frac{1}{4} \frac{\phi}{\rho_s} \frac{f_{ct}}{\tau_{bm}}$$

and, introducing for the bond stress the resisting value $f_b = \beta_b f_{ct}$ introduced in Sect. 1.4.3, one therefore has

$$\lambda = \frac{1}{4} \frac{\phi}{\rho_s} \frac{1}{\beta_b}$$

where β_b is the effective contact ratio.

The distance between adjacent cracks is greater for big bar diameters and for small reinforcement ratios. Even the bond parameter β_b has an influence on the spacing λ , which is smaller for ribbed bars with respect to the smooth ones.

In order to determine the crack width w , with a simplified formulation which assumes an elastic behaviour of the materials and approximates the diffusion of stresses according to the models presented above, one can calculate the difference between the elongation of the bar and the elongation of the concrete between two cracks that delimits the segment of Fig. 2.12. One therefore has, with obvious meaning of symbols:

$$w = 2(\Delta\lambda_s - \Delta\lambda_c)$$

with

$$\begin{aligned}\Delta\lambda_s &= \int_0^\lambda \frac{\sigma_s(x)}{E_s} dx = \frac{\sigma'_s + \sigma_s}{2E_s} \lambda = \frac{2\sigma'_s - \Delta\sigma_s}{2E_s} \lambda \\ \Delta\lambda_c &= \int_0^\lambda \frac{\sigma_c(x)}{E_c} dx = \frac{f_{ct}}{2E_c} \lambda\end{aligned}$$

The second contribution is small, given the low mean value $f_{ct}/2$ of stresses and it is uncertain in relation to the actual distribution of stresses in the concrete segment. Therefore, neglecting the concrete strain, the crack with w_{om} relative to a segment of unit length is given by the mean value of the strain of the steel bar:

$$w_{om} = \varepsilon_{sm} = \frac{\Delta\lambda_s}{\lambda} = \frac{\sigma'_s}{E_s} - \frac{1}{2} \frac{\Delta\sigma'_s}{E_s} = \frac{\sigma'_s}{E_s} - \frac{f_{ct}}{2\rho_s E_s}$$

In this expression of strain, the first contribution represents the one of bare bar, the second contribution represents the stiffening effect of concrete in tension between the cracks (“tension stiffening”).

It is to be noted that the summation of the widths of all cracks within a unit segment of a fully cracked tie does not depend on the crack spacing λ , but only on the stress in the bar calculated with the assumption of cracked sections, on the reinforcement ratio and on the tensile strength of concrete. Therefore, with the above-mentioned parameters unchanged, a greater crack spacing implies greater crack widths and vice versa.

In order to limit the crack *unit width* $w_{om} = \varepsilon_{sm}$, the stress in steel should be limited and concrete quality should be enhanced. In order to limit the *crack width*

$$w = w_{om}s$$

that is the width of individual cracks, ribbed bars and small diameters should also be used. The reinforcement ratio plays opposite roles: high ratio causes a greater but

more diffused cracking, with the diffusion effect prevailing which contributes to limit the width of individual cracks.

This formulation, based on much simplified theoretical assumptions, should be assumed as correct qualitative indication on the influence of the main parameters involved. It neglects certain important aspects of the phenomenon, such as the effects of the distribution of bars in the cross section. For a better quantification of the results, further deeper investigations should be carried, also with reference to the results of the experimental tests, as developed in the following chapter.

Eventually, the influence of other factor should be considered, such as the weakening of the sections in tension due to the stirrups, for which often the crack spacing corresponds to the spacing of the stirrups.

2.3 Cracking Calculations

With respect to the cracking verifications, structures can be in one of the following states:

- *cracked state in tension* if, even under a rare loading condition, the analysis of actions shows that the tensile concrete strength is exceeded;
- *uncracked state in tension* if this does not happen, not being able to exclude isolated cracks (e.g. due to shrinkage) which tend to open under tensile stresses, even if verified in the design under the tensile strength limit;
- *full compression state* (or, in less stringent terms, in low tension) where the absence of cracks is guaranteed.

The three states are defined by two limits:

- *the cracks formation limit* corresponding to the attainment of the tensile concrete strength ($\sigma_c = f_{ctk}$) in the uncracked section;
- *the decompression limit* corresponding to the zeroing of stresses ($\sigma_c = 0$) or, in less stringent terms, to the attainment of a very small tension limit (e.g. $\sigma_c = 0.25f_{ctk}$) in the uncracked section.

In the cracked state, the resistance verifications shall be carried with the usual assumption of cracked sections, and the cracking verifications are addressed to the calculation of the width w according to the models specified hereafter for the full stabilized cracked stage of the tie. In the uncracked state in tension, the resistance verifications shall again be related to the cracked section, whereas the verifications of the crack width, where required, should be related to the possible isolated crack. In the full compression state the section remains uncracked while obviously no crack width verification is required.

With reference to their width w , one can indicatively distinguish:

- *capillary cracks* with $0.0 < w < 0.2$ mm (not visible to the naked eye, to be measured with special magnifying glasses);

- *small cracks* with $0.2 < w < 0.4$ mm (visible to the naked eye but not evident);
- *big cracks* with $0.4 < w < 0.8$ mm (evident if not covered by plaster or other coating).

Bigger cracks represent serious static damages. They should therefore be excluded in the design; if identified in existing structures, they should be verified, as they can indicate the beginning of the failure of bond or also the yielding of the reinforcement, and could require repairs, strengthening or remakings, or at least the application of protective coatings. At Sect. 2.3.3, after the description of the models for the calculation of the crack width, the relative verification criteria will be summarized in details.

2.3.1 The Cracking Process

When cracking arises, the reinforced concrete tie assumes the deformed shape indicated by the detail of Fig. 2.13. The fact that tensions reach zero value at the cracks locations generates an extensive unloading in concrete which, segment by segment, tends to shrink. At the same time the reinforcing bar, under the complementary increase in stresses, tends to lengthen more with respect to the previous configuration of uncracked cross sections. After an initial settlement δ corresponding

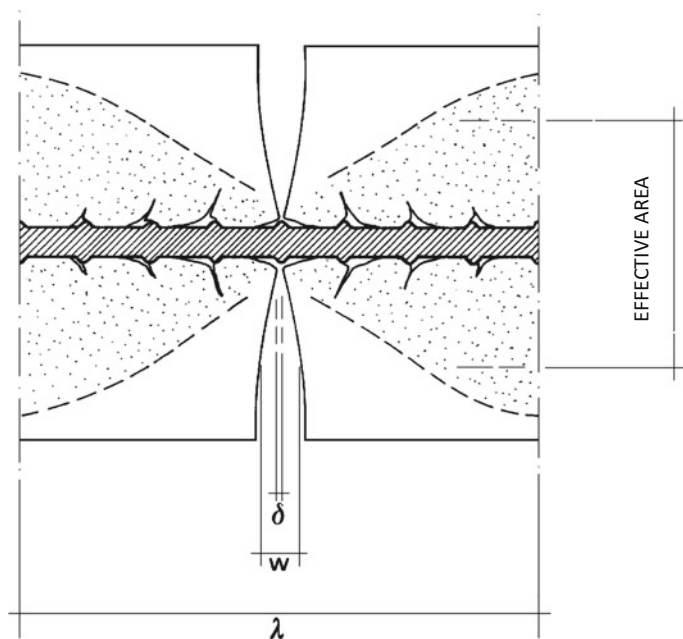


Fig. 2.13 Crack width

to the activation of the effective contacts, the relative slippage of the two materials is contrasted by bond. Thanks to this, part of the tensile force N in the tie, which is entirely concentrated in the reinforcing bar at the crack location, is diffused in the concrete segments as shown qualitatively with the dotted zones in Fig. 2.13. However, the gradual diffusion of stresses leaves concrete zones that are substantially unstressed, with a deformed shape of the segments which does not correspond anymore to plane sections. As indicated in Fig. 2.13, the crack itself is characterized by variable width, increasing with the distance from the reinforcement.

The phenomenon is approximated in the design, assuming an average behaviour through the segments, where the partial diffusion of stresses in concrete is represented by an effective area, reduced with respect to the actual area of the cross section, which depends on the position and distribution of the reinforcing bars. From these calculations a conventional value w of the crack width derives, on which verifications are empirically calibrated. However, these verifications are largely approximated because of the intrinsic difficulties of synthesizing in practical formulas the influence of numerous parameters in the various construction arrangements.

The overall behaviour of the tie, extended beyond the cracking limit, can be experimentally tested with the set-up of Fig. 2.14, measuring the elongation Δl . Correlating the values of the force N to the average elongation

$$\varepsilon_{sm} = \frac{\Delta l}{l}$$

of the bar, diagrams similar to the one shown in Fig. 2.15 are obtained.

The curve of the experimental behaviour of the tie is therefore characterized by:

- segment OA uncracked up to the tensile failure limit of concrete, with a substantially linear trend that follows the straight line (with $\sigma_c = E_c \varepsilon$, $A_i = A_c + \alpha_c A_s$ e $\psi_s = \alpha_c A_s / A_c$):

$$N = \sigma_c A_i = \frac{1 + \psi_s}{\psi_s} A_s E_s \varepsilon$$

- segment AB corresponding to the full cracking of the tie, with sudden reduction of the apparent stiffness due to the release of stresses in concrete and to the slippage of activation of bond contacts;

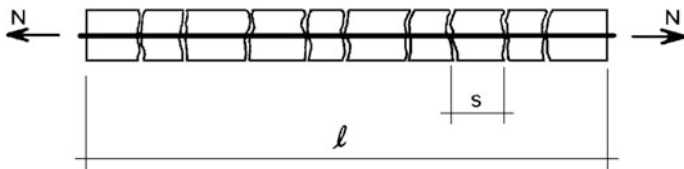


Fig. 2.14 RC tie—crack state

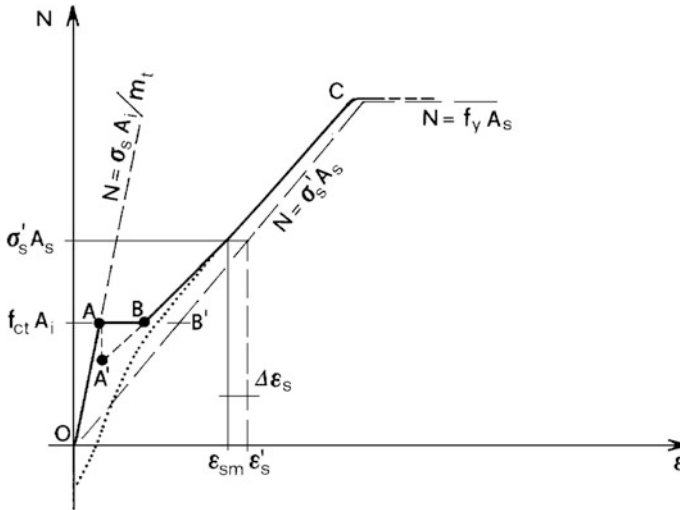


Fig. 2.15 Cracking of a RC tie—stress—strain diagram

- if the release of stresses in concrete was complete, the test would stabilize on the point B' of the line

$$N = \sigma'_s A_s = E_s A_s \epsilon'_s$$

- whereas the segment BB' represents the tension stiffening, that is the stiffening effect given by the segments of concrete in tension between the cracks;
- if the test was performed under displacement control, the segment $AA'B$ would follow, with the relaxation of force instead of the increase of deformation;
- segment BC , with decreasing contribution of the concrete in tension due to cracking and slippage, up to steel yielding.

When the tie is unloaded, the behaviour follows the dotted segment of Fig. 2.15. Cracks gradually close up bringing their width value w to zero. However, friction prevents the complete recovery of slippage δ : for $N = 0$ steel remains in tension, concrete in compression on average. Just with the application of a compression force N it is possible to bring the strain ϵ_s to zero.

2.3.2 Crack Width

The average strain of steel reinforcement can be therefore read from the diagram of Fig. 2.15 as:

$$\varepsilon_{sm} = \varepsilon'_s - \Delta\varepsilon_s$$

where $\varepsilon'_s = \sigma'_s/E_s$ is the strain of the bare bar subject to the full force N , and $\Delta\varepsilon_s$ is the effect of tension stiffening that has been expressed from the theoretical point of view at Sect. 2.2.3 as $f_{ct}/(2\rho_s E_s)$. It can be observed experimentally that such effect is not constant, but decreases as the load increases: the *hyperbolic model* shows good fit with the measured data, decreasing with the stress σ'_s . With reference to the diagram of the behaviour transposed on the variable $\sigma'_s = N/A_s$ (see Fig. 1.16), where σ'_s and $\Delta\bar{\varepsilon}_s$ correspond to the point D of the theoretical cracks closure, one can therefore set:

$$\Delta\varepsilon_s = \frac{\bar{\sigma}'_s}{\sigma'_s} \Delta\bar{\varepsilon}_s$$

With this model one has:

$$\varepsilon_{sm} = \varepsilon'_s - \frac{\bar{\sigma}'_s}{\sigma'_s} (\bar{\varepsilon}'_s - \bar{\varepsilon}_{sm})$$

which, with

$$\frac{\bar{\varepsilon}'_s}{\varepsilon'_s} = \frac{\bar{\sigma}'_s}{\sigma'_s}$$

leads to

$$\varepsilon_{sm} = \frac{\bar{\sigma}'_s}{\sigma'_s} \bar{\varepsilon}_{sm} + \varepsilon'_s \left[1 - \left(\frac{\bar{\sigma}'_s}{\sigma'_s} \right)^2 \right]$$

If the first term is assumed to represent the average concrete strain ε_{cm} , decreasing as the force goes up because of the loss of bond (see Fig. 2.16), the second represents the average reinforcement strain related to the strain of concrete and therefore indicates the average unit crack width:

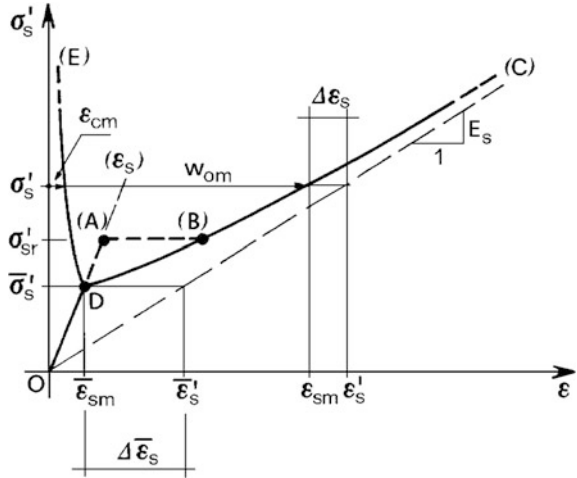
$$w_{om} = \varepsilon_{sm} - \varepsilon_{cm} = \frac{\sigma'_s}{E_s} \left[1 - \left(\frac{\bar{\sigma}'_s}{\sigma'_s} \right)^2 \right]$$

With reference to the reinforcement stress calculated in the cracked section for the force corresponding to the tensile rupture of concrete:

$$\sigma'_{sr} = \frac{N_r}{A_s} = \frac{A_i f_{ct}}{A_s}$$

one can approximately set the origin of the hyperbolic model in:

Fig. 2.16 Stress–strain cracking model



$$\bar{\sigma}'_s \cong 0.7\sqrt{\beta^*}\sigma'_{sr}$$

where the numerical coefficient represents the effect of the stress release in the concrete segments further to cracking and β^* synthesizes the influence of other main parameters:

$$\beta^* = \beta_0\beta_1\beta_2$$

where $\beta_0 (\leq 1.0)$ indicates the effective reinforcement ratio that takes into account the distribution of the bars in the cross section, β_1 corresponds to the bond parameter already defined as the effective contact ratio (assumed here equal to 1.0 for ribbed bars, 0.5 for smooth bars), β_2 simulates the effects of duration and cycles of loads ($=1.0$ for the first load application, $=0.5$ for loads of long duration or repeated).

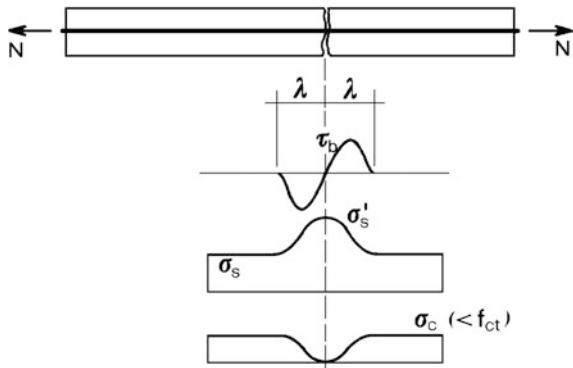
With those assumptions, the average unit crack width is given by

$$w_{om} \cong \frac{\sigma'_s}{E_s} \left[1 - 0.5\beta_0\beta_1\beta_2 \left(\frac{\sigma'_{sr}}{\sigma'_s} \right)^2 \right] \quad \text{for } \sigma'_s > \bar{\sigma}'_s$$

$$w_{om} = 0 \quad \text{for } \sigma'_s \leq \bar{\sigma}'_s$$

It is to be noted that for prestressed ties, the average strain of reinforcement should be measured from the decompression of concrete. The stress σ'_s should therefore be replaced with the value $\sigma'_p - \sigma_{po}$.

Assuming now that the crack spacing varies between λ and 2λ , the crack width would therefore vary from

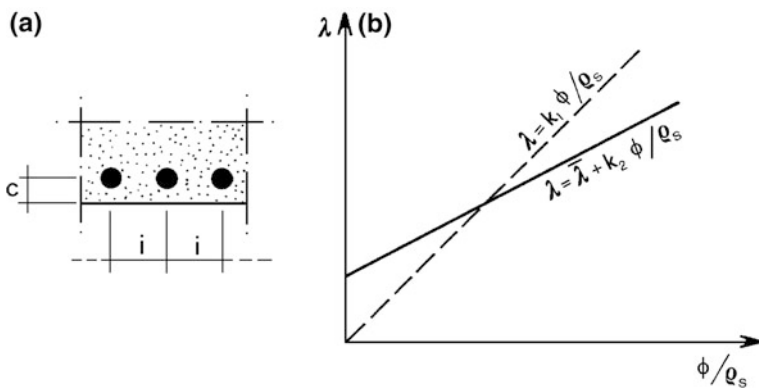
Fig. 2.17 Stress distribution around an isolated crack

$$w = \lambda w_{om} \quad \text{to} \quad w = 2\lambda w_{om}$$

In particular, for $\bar{\sigma}'_s < \sigma'_s < \sigma_{sr}$, the single crack width (see Fig. 2.17) is to be evaluated as

$$w = 2\lambda w_{om}$$

In Sect. 2.2.3 a formulation of λ has been given, with a simplified theoretical formulation, as a function of the bars diameter, the reinforcement ratio and the bond parameter. Experimental tests correct this expression with a binomial formula that also takes into account the edge distance c measured to the reinforcement centreline (see Fig. 2.18a):

**Fig. 2.18** Models for crack spacing

$$\lambda = c_o + \frac{0.1}{\beta_1} \left(\frac{\phi}{\rho_s} \right)$$

with $c_o = c - \phi/2$.

In this formula, the reinforcement ratio ρ_s should refer to the effective area consisting of a strip of thickness equal to $2.5c$. The two curves $\lambda = \lambda(\phi/\rho_s)$ are shown in Fig. 2.18b, the binomial empirical one with a solid line, the simplified theoretical one with a dashed line.

The formula of crack spacing shown above refers to the concrete layer surrounding the bar, with a width roughly equal to 5ϕ , which gives its protective cover against corrosion. When the spacing i between bars (see Fig. 2.18a) is largely greater than this value ($i \gg 5\phi$), in the intermediate portions a different cracking pattern occurs, characterized by a greater spacing, close to the transverse dimension of the element, and by a width of individual cracks proportionally greater. The concentration of width in few largely spaced cracks, even though it does not compromise the protection of reinforcement bars, can have negative aesthetic consequences because of the evidence of the phenomenon to the naked eye.

It is to be noted how the adopted model, with its point D (see Fig. 2.16), introduces a new limit state that is the one of (theoretical) *cracks re-closure*, which can be calculated equating stress $\sigma'_s = N/A_s$ to the value $\bar{\sigma}'_s$ defined above.

In Sect. 3.3 it will be also shown how, from the hyperbolic models of tension stiffening, a law of deformation of cracked sections can be deduced, with reference both to the axial deformations of ties and to the flexural curvatures of beams.

2.3.3 Verification Criteria

If well executed, respecting chemical requirements and technological prescriptions, concrete offers a good protection to reinforcement. The structural designer is responsible for the correct indication of the reinforcement position and the cracking verification.

The external concrete layer is subject to progressive carbonation along the time. This concerns indicatively a depth between 15 and 25 mm, beyond which the phenomenon is significantly reduced. Carbonation is the cause that triggers the oxidation process of steel. An adequate cover therefore has to be provided, otherwise oxidation starts and progressively extends, often with bulges, with consequent spalling and direct exposure of the reinforcement.

An excessive cracking opens the way for a deeper penetration of the phenomenon, whereas its speed of propagation is mainly related to three parameters:

- the *aggressiveness conditions* of the environment;
- the *percent duration* of exposure in the foreseen cracked state;
- the *sensitivity* of reinforcement to corrosion.

Apart from the more detailed indications of Table 2.1, the environments can be summarized into:

- *slightly aggressive*, ordinary environments with small humidity range (Classes: X0, XC1, XC2 and XC3 of Table 2.1);
- *moderately aggressive*, tidal, splash and spray zones or exposed to airborne salt (Classes: XD1 and XS1 of Table 2.1);
- *highly aggressive*, chlorides or sea waters (Classes: XD2, XD3, XS2 and XS3 of Table 2.1).

The percent duration of exposure is conventionally assumed in the different loads combinations:

- *rare*,
- *frequent*,
- *quasi-permanent*.

Concerning the propagation speed of the corrosion effects with respect to the initial strength, two types of reinforcement can be distinguished:

- *slightly sensitive*,
- *sensitive*,

the latter consisting in: small diameters ($\phi \leq 4$ mm), for which a given depth of oxidation has a high percent influence on the resisting cross section; tempered bars that exhibit surface microcracks, due to the thermal treatment undergone, open to a deeper penetration of corrosion; cold-hardened bars, in which surface microcracks open up under high tensile stresses ($\sigma_s > 390$ MPa).

Direct Analytical Criterion

The summary outline of the cracking verification criteria based on the calculation of crack width w can therefore be presented as indicated in the following table. The admissible limits of the width w_k correspond to $\bar{w}_1 = 0.2$ mm, $\bar{w}_2 = 0.3$ mm, $\bar{w}_3 = 0.4$ mm.

For the verification of crack openings according to the semi-probabilistic method, the conventional procedure is followed which assumes a characteristic value of the distance between cracks equal to

$$s_k = 2\lambda$$

and a characteristic value of the average unit width equal to

$$w_{ok} = kw_{om}$$

with $k = 1.7$.

The conventional width for the verifications is therefore obtained as:

$$w_k = s_k w_{ok}$$

and it shall be lower than the limit values \bar{w}_i shown in the table.

Reinforce sensitivity	Environ. aggressive	State	Load combination	Verification	w_k
Slightly sensitive	Low	Cracked	Rare	—	—
			Frequent	Crack width	\bar{w}_3
			Quasi perm.	”	\bar{w}_2
	Medium	Cracked	Rare	—	—
			Frequent	Crack width	\bar{w}_2
			Quasi perm.	”	\bar{w}_1
	High	Cracked	Rare	—	—
			Frequent	Crack width	\bar{w}_1
			Quasi perm.	Re-closure	0
Sensitive	Low	Cracked	Rare	—	—
			Frequent	Crack width	\bar{w}_2
			Quasi perm.	”	\bar{w}_1
	Medium	Uncracked	Rare	Crack formation	—
			Frequent	Crack width	\bar{w}_1^*
			Quasi perm.	Re-closure	0*
	Medium	Uncracked	Rare	Crack formation	\bar{w}_1^*
			Frequent	Re-closure	0*
			Quasi perm.	Decompression	—

*Is referred to the width of the single isolated crack

Indirect Technical Criterion

The previous verification criterion, based on the analytical calculation of the crack width, appears to be conceptually correct. From the applicative point of view it is less effective because of the low accuracy of the formulas. Through the articulated verification workflow one arrives to an evaluation downgraded because of the modest precision of the elaborated data.

Currently, waiting for more reliable calculation models, the technical criterion that approximates certain parameters is in general preferable, which therefore also simplifies the verification of crack width, reducing it to a check of the stress level in the reinforcement.

The technical criterion is based on certain assumptions about the domain of validity and the limits of the concerned parameters:

- for the cracking unit width $w_{om} = \varepsilon'_s(1 - \kappa)$ with ribbed bars well distributed and under loads of long duration or repeated ($\beta_o = 1.0$, $\beta_1 = 1.0$ and $\beta_2 = 0.5$) a

variable stiffening contribution is assumed with σ'_{sr}/σ'_s indicatively from $\kappa \cong 0.25$ to $\kappa \cong 0.05$;

- requirements on the amount and distribution of reinforcement are imposed, for example with a distance between the bars $i \leq 5.0\phi$, to which a given empirical effective reinforcement ratio ρ^* corresponds;
- an average value of cover for longitudinal bars is assumed, for example with $c_o \cong 25$ mm.

Consequently, the cracks maximum spacing and the unit width are evaluated as a function of the bars diameter and the stress in steel (with $k = 1.7$):

$$s_k = 2\lambda = 2\left(c_o + \frac{0.1}{\beta_1} \frac{\phi}{\rho_s^*}\right) \cong 50 + 0.2 \frac{\phi}{\rho_s^*}$$

$$w_{ok} = k \frac{\sigma'_s}{E_s} (1 - \kappa) = \sigma'_s [1 - \kappa(\sigma'_s)] / 120000$$

Equating the expression of the crack width to the corresponding admissible limit value

$$w_k = s_k w_{ok} = \bar{w}_i$$

for the stress σ'_s calculated in the cracked section under the characteristic action of the pertinent load combination, the corresponding admissible value is eventually obtained with

$$\bar{\sigma}'_s = \sigma'_s(\bar{w}_i, \phi)$$

Based on these criteria, the tables of *admissible stresses* are given which, in the specified limits of applicability, implicitly satisfy the cracking width verifications.

For reinforcements sensitive to corrosion in environments mid or highly aggressive, the additional verifications for crack formation and decompression limit states are required under the appropriate loads combinations, whereas the verification of cracking re-closure is carried, still in terms of admissible stresses in steel, with $\sigma_s < \bar{\sigma}'_s$ (see Fig. 2.16).

The scheme of the verifications for ties according to the criteria mentioned above, in addition to the relative tables of admissible stresses, is shown in Chart 2.15 and Table 2.16.

Minimum Reinforcement

The cracking calculations presented here refers to the effects of static actions that are explicit tensile forces applied on the tie. Significant effects can also derive from geometrical actions such as shrinkage and thermal variations. The consequent self-induced stresses are added to the effects of external loads and, especially for redundant concrete sections, where the calculations lead to small reinforcement ratios, can cause excessive cracking.

Since self-induced stresses tend to extinguish when cracking arises, the adopted criterion consists of guaranteeing, independently from the external loads, a minimum amount of reinforcement capable of absorbing, at the yielding limit, the tensile force released by concrete when cracking:

$$A_s \geq A_c f_{ctm} / f_{yk}$$

With common materials this formula gives minimum reinforcement of about 0.7%.

2.4 Case A: RC Multi-storey Building

A first example of building on which numerical applications of the verification calculations are performed is represented by the multi-storey building whose typical plan and section are shown in Figs. 2.19 and 2.21. It is a building of five storeys above ground with one basement level, with a rectangular plan, for residential use. The structural layout reflects a common typology, with some simplification of the layout with respect to the possible real configurations. This is with the aim of making easier the derivation of static schemes from the structural context.

A traditional cast in situ concrete building is assumed. The decks are made of clay blocks with interposed reinforced concrete ribs and a collaborating topping (see Fig. 2.22). The floor is spanning in the transverse direction with respect to the main side of the building and it is supported by three longitudinal beams, two edge beams within the floor thickness and a central deeper beam. There are transverse ribs to connect the main ones, in order to adequately distribute possible concentrate loads among them. At the two lateral edges the floors end with beams, more reinforced than the typical ribs, supporting the dead load of the cladding walls located there.

The edge beams consist of a solid strip of concrete, of the same thickness of the floor, containing the appropriate reinforcement. They sit on the corresponding row of columns, forming with these a supporting frame, resisting the actions coming from floors and the loads directly applied on the beams, such as the weight of the cladding walls. In the case under consideration the central beam is deeper than the floor, with a web that, together with the solid strip in the floor thickness, gives it the T shape. In addition to the internal row of columns, this beam sits on the walls of the staircase which, placed in a central position, splits it into two pieces, same as the edge beam of the inner façade.

The reinforced concrete walls of the staircase form a very rigid box structure. The lateral stability of the building relies on this central core to resist the expected horizontal forces. In Sect. 8.4 the analysis of the overall structural behaviour with respect to its global stability will be further developed. For now it is important to highlight how, with the horizontal elements connected to the central stability core, the individual vertical frames of the structure can be considered as non-sway frames: the small horizontal displacements allowed at different levels by the high

stiffness of the stability core have negligible effects on the other much flexible elements such as beams and columns.

From the synthetic description of works, it is clear that the multi-storey structure under analysis consists of a complex three-dimensional frame. In what follows the analysis of some elements of this frame will be performed, with approximated procedures based on the extraction of appropriate partial static schemes, mainly reduced to plane models of flexural behaviour. The global three-dimensional analysis would lead to an onerous calculation due to the high degree of redundancy of the structure. For a correct evaluation of internal forces, the variability of the structural configuration itself, further to the sequence of the execution stages of construction, should be taken into account. If set-up according to precise criteria that keep under control the degree of approximations introduced and their reliability limits with respect to safety, the simplified procedures give good technical solutions for the verification problems.

In the calculations that follow, reference is made to the European norm EN 1992-1-1:2004 “Eurocode 2: Design of Concrete Structures—Part 1: General rules and rules for buildings”.

For the execution and functional purposes the structural layout is described in the *Design Documentation*, in which the structural designer transposes its work. This documentation consists of the *Construction Drawings* which will lead the execution on site and the *Design Report* which shows the analysis and the design calculations of the structures.

More details about the design report will be given in Sect. 3.4 of the following chapter. Certain general indications about the construction drawings are given here that should be considered only indicative since there can be significant variations based on the different structural typologies and the size of the works.

Usually, the basic reference is the overall design of the building described by *Drawings “A”* of the Architectural Design that give the *architectural arrangement* of the building, and by the relative *Drawings “B”* with the *construction details* of the works. For the structures, the competent designer should provide the *Drawings “C”* with indicated the general dimensions and the details of the concrete elements, as well as the *Drawings “D”* with the *reinforcement* detailing. For a building like the one examined in these pages, one can have, for example the following drawings (usually numbered in the order in which they are used on site according to the sequence of the works):

DRAWINGS “C” OF GENERAL ARRANGEMENT

- DWG. C.1—Foundation Layout
- DWG. C.2—Ground Floor Layout
- DWG. C.3—Type Floor Layout
- DWG. C.4—Roof Layout
- DWG. C.5—General Sections

DRAWINGS “D” OF REINFORCEMENT

- DWG. D.1—Foundation Details

DWG. D.2—Columns Tables
 DWG. D.3—Ground Floor Slabs
 DWG. D.4—Ground Floor Beams
 DWG. D.5—Type Floor Slabs
 DWG. D.6—Type Floor Beams
 DWG. D.7—Roof Slabs
 DWG. D.8—Roof Beams
 DWG. D.9—Corewall
 DWG. D10—Staircases Details

Sometimes, not for big constructions, the layout of the slabs reinforcement is directly incorporated in the General Arrangement drawing of the relative floor. Drawings of the type D.3, D.5 and D.7 can therefore be missing and the three concerned General Arrangement drawings can become:

DWG. CD.2—Ground Floor Layout and Slabs Reinforcement
 DWG. CD.3—Type Floor Layout and Slabs Reinforcement
 DWG. CD.4—Roof Layout and Slabs Reinforcement

Following the design applications, a few examples of construction drawings are shown in this volume, both for the General Arrangement (see Figs. 2.19, 2.20 and 12), and for the reinforcement (see Figs. 2.24, 3.48, 4.45, 5.50, 6.45, 8.25, 8.26, 8.31, 9.50, 9.51).

2.4.1 Actions on Columns and Preliminary Verifications

Analysis of Loads

For the analysis of loads applied on the bearing structure of the building, other than the dimensions of the structures themselves, finishes and occupancy as derived from the architectural design have to be considered. In these pages only a few construction elements are described, to show common examples of loads estimation. In Fig. 2.21 the different layers of the main types of walls are therefore indicated: the double external wall for the outer envelope of the building and the simple wall for internal partitions. Gravity loads are obviously evaluated as the product of volume and unit weight.

Double external wall

• external plaster	0.03×20	$= 0.60$	kN/m^2
• external hollow bricks	0.12×16	$\cong 1.90$	”
• rough plaster	0.02×20	$= 0.40$	”
• thermal insulation	0.03×1	$\cong 0.05$	”
• internal brickwork	0.06×11	$\cong 0.65$	”
• internal plaster	0.02×20	$= 0.40$	”
• tot per unit area of wall		$= 4.00$	kN/m^2

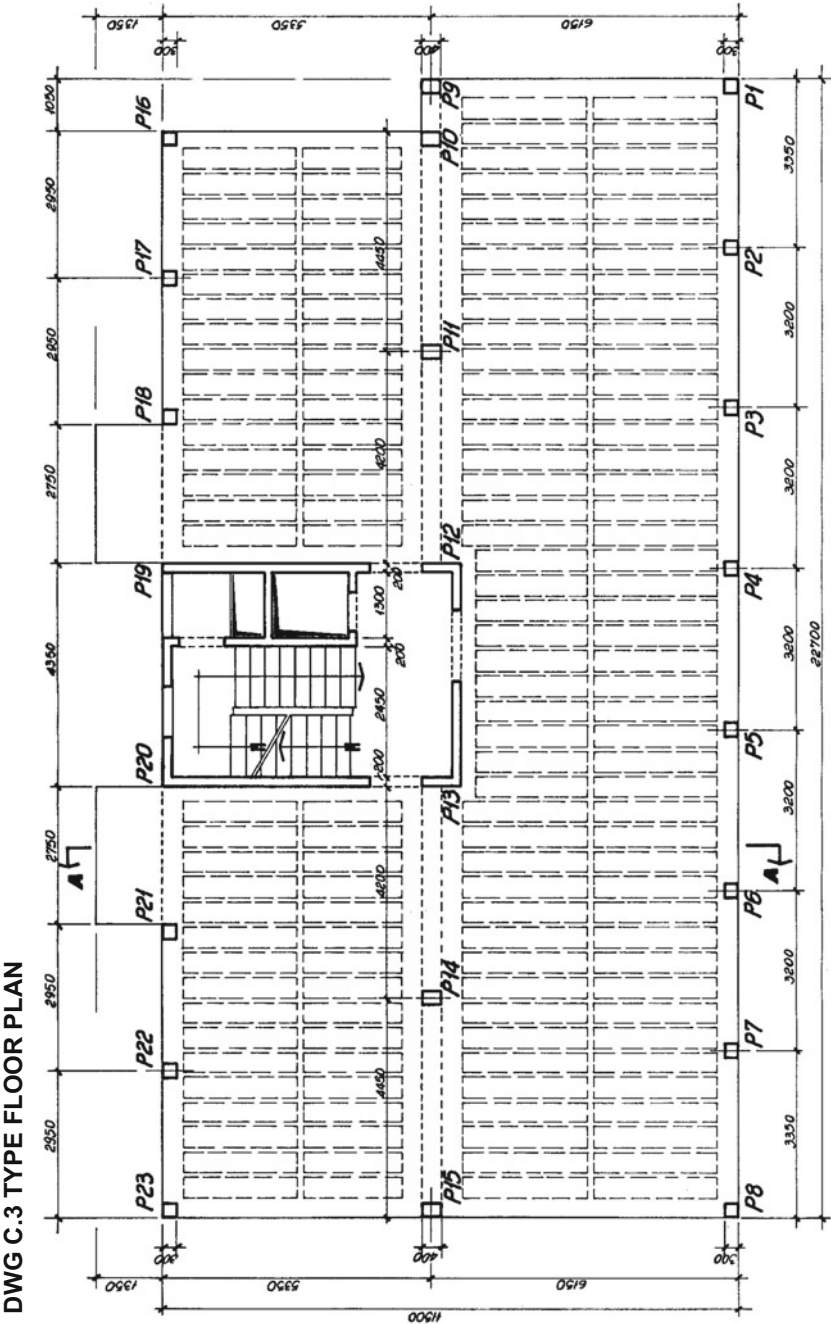


Fig. 2.19 Multistorey building—plan

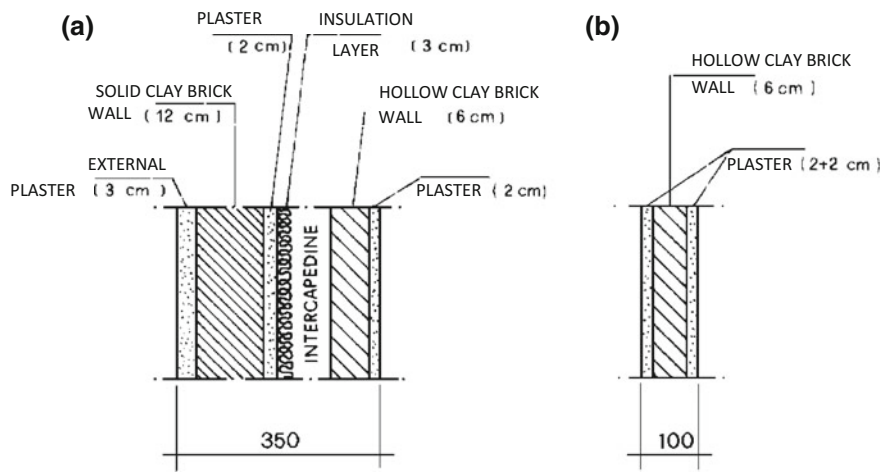


Fig. 2.21 Details of cladding (a) and partitioning (b) walls

Average dead load
(clear headroom $3.06 - 0.24 = 2.82$ m)

• walls	2.82×4.00	$\cong 11.30$	kN/m
• openings incidence	-0.2×11.30	$\cong -2.30$	kN/m
at floor level per unit length of wall		$= 9.00$	kN/m

Simple partition

• plasters	$2 \times 0.02 \times 20$	$= 0.80$	kN/m ²
• brickwork	0.06×11	$\cong 0.65$	kN/m ²
tot per unit area of wall		$= 1.45$	kN/m ²
per unit length of wall	1.45×2.82	$= 4.09$	kN/m

Average dead load

• average load on plan $4.09/2.5$	$= 1.64$	kN/m ²
• rounding	$= 0.36$	kN/m ²
tot per unit area of deck	$= 2.00$	kN/m ²

For what concerns the floors one can refer to the detail of Fig. 2.22 and to the dimensions of the deck shown in Fig. 2.19.

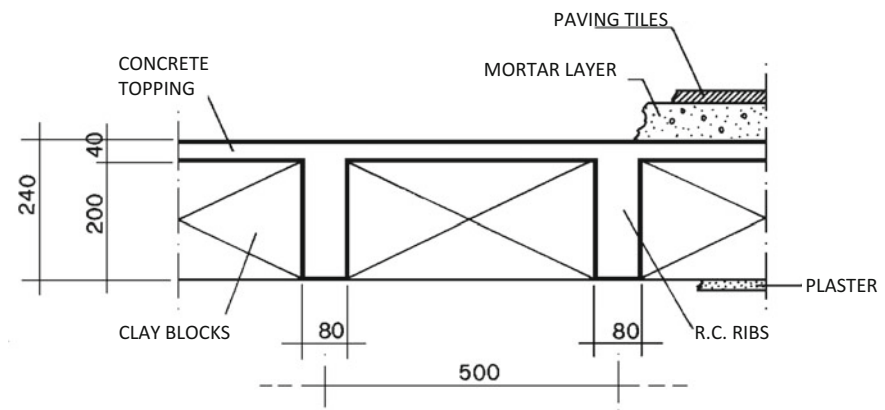


Fig. 2.22 Details of the floor

Type floor

• RC top slab	0.04×25	$= 1.00$	kN/m^2
• RC ribs	$0.20 \times 25 \times 8/50$	$= 0.80$	"
• hollow blocks	$0.20 \times 4^*$	$= 0.80$	"
tot per unit area of floor		$= 2.60$	kN/m^2

(*unit weight of hollow clay blocks $\cong 40 \text{ N/cm per square metre}$)

Average dead load

• current floor self weight		$= 2.60$	kN/m^2
• incidence of solid ribs	$(6.0 - 2.6) \times 225/1150$	$\cong 0.65$	"
• tot deck self weight		$= 3.25$	kN/m^2
• flooring		$= 0.40$	"
• screed (lightweight c.)	0.06×16	$\cong 0.95$	"
• plaster	0.02×20	$= 0.40$	"
• distributed partitions		$= 2.00$	"
tot permanent per unit area on plan		$= 7.00$	kN/m^2

Variable loads

- live loads (residential) $= 2.00 \text{ kN/m}^2$

For the roof a structure made of thin plates and bearing walls is assumed, sitting directly on the last horizontal floor, to form the slope of the pitched roof and an upper layer of common interlocking shingles.

Roof floor

• shingles	$1.1^{\wedge} \times 0.60 \cong 0.65$	kN/m^2
• thin plates	$1.1 \times 0.35 \cong 0.40$	kN/m^2
• distributed bearing walls	$1.5 \times 0.65 \cong 1.00$	kN/m^2
• screed in lightweight concr.	$0.08 \times 16 \cong 1.25$	kN/m^2
• thermal insulation	$0.03 \times 1 \cong 0.05$	kN/m^2
• floor self-weight	$= 3.25$	kN/m^2
• plaster	$0.02 \times 20 = \underline{0.04}$	kN/m^2
tot permanent per unit area on plan	$= 7.00$	kN/m^2

(\wedge projection of the pitched roof on plan)

Variable loads (snow)

(Zone 1, altitude $a_s < 200$ m, roof slope $\alpha < 30^\circ$ with $\mu_d = 0.8$)

- variable load $0.8 \times 1.5 = 1.20 \text{ kN/m}^2$

For the verification of column, variable loads at different floors of the building are assumed to occur with reduced intensity according to what is given in thecharacteristic combination***:

- top floor $1.0Q_o$
- lower floors $0.5Q_o + 1.0Q_1 + 0.7Q_2 + 0.7Q_3 + 0.7Q_4 \dots$

with Q_o snow load on the roof and $Q_1, Q_2, \dots, Q_i, \dots$ variable loads at residential floors numbered from top to bottom. In the case of concern one therefore has, with a unique load combination:

• roof	1.0×1.20	$= 1.20$	kN/m^2
• 4th floor	$1.0 \times 2.00 - 0.5 \times 1.20$	$= 1.40$	”
• lower floors	0.7×2.00	$= 1.40$	”

Actions on Columns

For the preliminary design of the columns, with reservation of farther verifications after more rigorous analyses of the frames, an approximated procedure can be followed based on the partition of the deck layout in *tributary areas*. This is obtained marking on such layout the mid-span lines of each individual span for slabs and beams in order to identify the loading areas to be attributed to each column (see Fig. 2.23). Apart from special situation, for example adjacent spans of very different

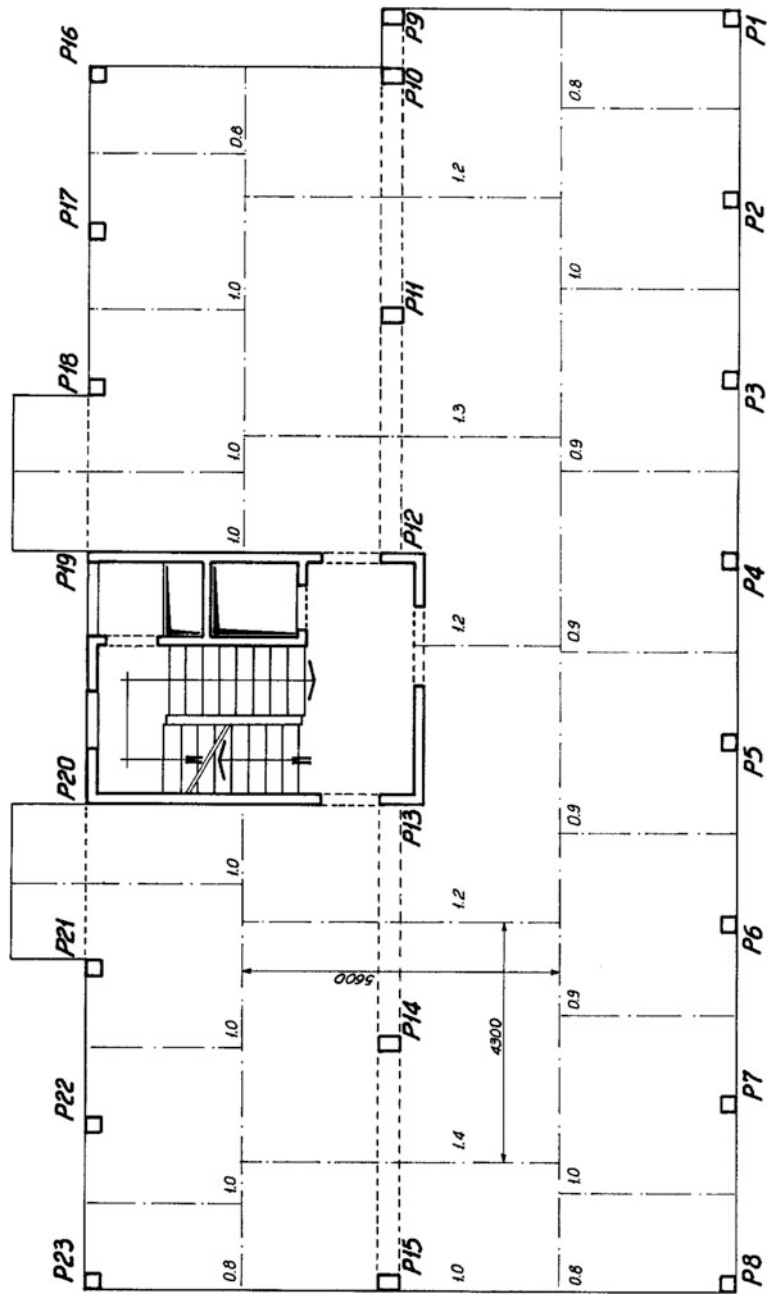


Fig. 2.23 Tributary areas of columns

length, it is possible to carry out an approximated evaluation of the effects of hyperstatic bending moments due to continuity of flexural elements, penalizing certain areas with amplifying coefficients and reducing others at the same time. For the case under analysis this has been done with *weights* indicated inside each individual tributary area, where for example the increase of the floor reaction on the intermediate support given by the central beam has been estimated with 0.2, combining it with similar estimations on the orthogonal flexural behaviour of the beam.

After carrying out such partition, one can proceed with the estimation of loads for each individual column, or by groups of similar area, eventually summing up forces from the top to the bottom with the combination formula indicated above. The calculation is developed below with reference to one column only.

Column P14

(tributary area	$1.4 \times 4.30 \times 5.60 \cong 33.7 \text{ m}^2$)		
• roof deck	33.7×7.00	$= 235.9$	kN
• beam	$1.2 \times 0.40 \times 0.30 \times 4.30 \times 25$	$= 15.5$	"
• column	$0.40 \times 0.30 \times 2.52'' \times 25$	$= \underline{7.6}$	"
total permanent loads on the roof		$= 259.0$	kN

(" clear headroom underneath the beam = 2.52 m)

• type floor deck	33.7×7.00	$= 235.9$	kN
• beam	$1.2 \times 0.40 \times 0.30 \times 4.30 \times 25$	$= 15.5$	"
• column [°]	$0.40 \times 0.40 \times 2.52 \times 25$	$= \underline{10.1}$	"
tot. permanent loads on type floor		$= 261.5$	kN

([°] average dimensions)

Roof

• permanent	$= 259.0$	kN
• variable 33.7×1.20	$= \underline{44.4}$	"
tot. roof	$= 299.4$	kN

4th floor

• permanent	$= 261.5$	kN
• variable 33.7×1.40	$= \underline{47.2}$	"
tot 4th floor	$= 308.7$	kN

lower floors

• permanent	= 261.5	kN
• variable 33.7×1.40	= <u>47.2</u>	"
tot lower floors	= 308.7	kN

After this preliminary analysis, the design calculations of sections and the service and ultimate limit state verifications can be neatly summarized as indicated in the following tables. The characteristics of materials assumed for the verifications are shown below.

Materials

Concrete (aggregate $d_a \leq 20$ mm)

• class C25/30 ordinary ($R_{cm} \cong 40$ N/mm ²)		
• characteristic strength	f_{ck}	= 25.0 N/mm ²
• design strength	$f_{cd} = 0.85 \times 25.0/1.5$	= 14.2 N/mm ²
• for centred axial force	$f'_{cd} = 0.80 \times 14.2$	= 11.3 N/mm ²
• allowable in service	$\bar{\sigma}_c = 0.45 \times 25.0$	= 11.2 N/mm ²
• for centred axial force	$\bar{\sigma}'_c = 0.70 \times 11.2$	= 7.8 N/mm ²

Steel (ribbed bars)

• type B450C with high ductility		
• characteristic strength	f_{tk}	= 540 N/mm ²
• yield stress	f_{yk}	= 450 N/mm ²
• design strength	$f_{yd} = 450/1.15$	= 391 N/mm ²
• allowable in service	$\bar{\sigma}_s$	= $0.80 \times 450 = 360$ N/mm ²

Homogenization coefficients

- for serviceability design $\alpha_e^* = 15$
- for ultimate design $391/11.3 = 34.6$

It is to be noted that, as permitted by the codes, for the elastic design a conventional homogenization coefficient is assumed which takes into account the creep effects produced by the permanent quota of loads in an approximated way. Given that this quota corresponds on average to 0.7 of the total loads, with a creep coefficient $\varphi \cong 2.4$ and with reference to an ordinary concrete with $\alpha_c \cong 7$, one obtains approximately:

$$\alpha_e^* \cong (1 + 0.70^2 \times 2.4) \cdot 7 \cong 15$$

This approximation does not affect significantly the evaluation of serviceability stresses in concrete, whereas it has no influence on the ultimate resistance of the sections.

Another approximation is made in the design of columns with the adoption of a global safety factor on actions, evaluated as the weighted mean between the factor $\gamma_{G1} = 1.30$ of structural dead loads and the one $\gamma_{G2} = \gamma_Q = 1.50$ of applied loads:

$$\gamma_F \cong 1.30 \times 0.35 + 1.50 \times 0.65 \cong 1.43$$

having estimated in 0.35 the incidence of structural dead loads on the total.

Verification Calculations

COLUMN P 14—SECTIONS DESIGN									
	F_k (kN)	N_k (kN)	N_{Ed} (kN)	A_{co} (cm ²)	$a \times b$ (cm)	A_c (cm ²)	A_{so} (cm ²)	$n\phi$ (mm)	A_s (cm ²)
4°	299.4	299.4	428.1	379	30 × 40	1200	3.60	4φ12	4.52
3°	308.7	608.1	869.6	770	30 × 40	1200	3.60	4φ12	4.52
2°	308.7	916.8	1311.0	1160	30 × 40	1200	3.60	4φ12	4.52
1°	308.7	1225.5	1752.5	1551	40 × 40	1600	4.80	4φ14	6.16
PR	308.7	1534.2	2193.9	1942	50 × 40	2000	6.00	4φ14 + 2φ12	8.42
SI	308.7	1842.9	2635.3	2332	60 × 40	2400	7.20	6φ14	9.24

COLUMN P 14 SECTIONS VERIFICATION					
	A_{ic} (cm ²)	σ_c (MPa)	A_{ir} (cm ²)	N_{Rd} (kN)	γ_r
4°	1268	2.4	1356	1532	3.58
3°	1268	4.8	1356	1532	1.76
2°	1268	7.2	1356	1532	1.17
1°	1692	7.4	1813	2049	1.17
PR	2008	7.6	2291	2589	1.18
SI	2539	7.3	2720	3074	1.17
		(≤ 7.8)			(≥ 1.00)

In the first table, from the last floor to the basement, the values of the following parameters are shown:

- The load F_k coming from the upper floor of the column considered.
- The axial force N_k obtained progressively summing up the upper loads.
- The design value of the axial force N_{Ed} obtained amplifying by $\gamma_F = 1.43$ the previous force.
- The minimum theoretical concrete area $A_{co} = N_{Ed}/f'_{cd}$ necessary to resist the design force by itself.
- The actual dimensions $a \times b$ adopted for the column segment.
- The actual concrete area A_c .

- The theoretical minimum reinforcement area $A_{so} = 0.10 \times N_{Ed}/f_{yd}$ equal to at least to the 0.3% of the actual concrete section A_c .
- The adopted reinforcement for the column segment indicated with the number n of bars and their diameter ϕ .
- The area A_s of the actual steel reinforcement cross section.

In the second table, again from the top floors to the bottom, the values of the following parameters are shown:

- The equivalent area $A_{ie} = A_c + \alpha_e A_s$ referred to concrete with the conventional homogenization coefficient $\alpha_e = 15$ for the serviceability elastic design.
- The stress $\sigma_c = N_k/A_{ie}$ in concrete for the serviceability compression verification, to be compared with the value 7.8 indicated at the bottom of the table column.
- The equivalent area $A_{ir} = A_c + A_s f_{yd}/f'_{cd}$ referred to concrete with the coefficient for the ultimate design of the section.
- The resisting value $N_{Rd} = f'_{cd} A_{ir}$ of the axial force to be compared with the applied value N_{Ed} .
- The ratio $\gamma_r = N_{Rd}/N_{Ed}$ between resistance and action in the section for a uniform comparison of the situations, having to satisfy $\gamma_r \geq 1$.

The transition from the design carried in the previous pages to the construction drawings with member detailing does not require explanations other than some short notes on certain code requirements, such as the one about spacing s and diameter ϕ_o of stirrups ($s \leq 12\phi$, $\phi_o \leq \phi/4$, where ϕ is the diameter of the longitudinal reinforcement). The relative DWG D.2 (Fig. 2.24) shows the column elevation, from the foundations to the roof, with the reinforcement indicated. On the side, the longitudinal bars are shown for the necessary dimensions. The lapping of bars specified at each floor at the location of the construction joints is to be noted. The different sections are eventually shown at a greater scale with the position of bars and the detailing of stirrups. Concerning the bars lapping, the minimum anchorage length has been used:

$$l_b = \frac{\phi f_{yd}}{4 f_{bd}}$$

With

$$f_{yd} = 391 \text{ N/mm}^2$$

$$f_{ctk} = 1.95 \text{ N/mm}^2$$

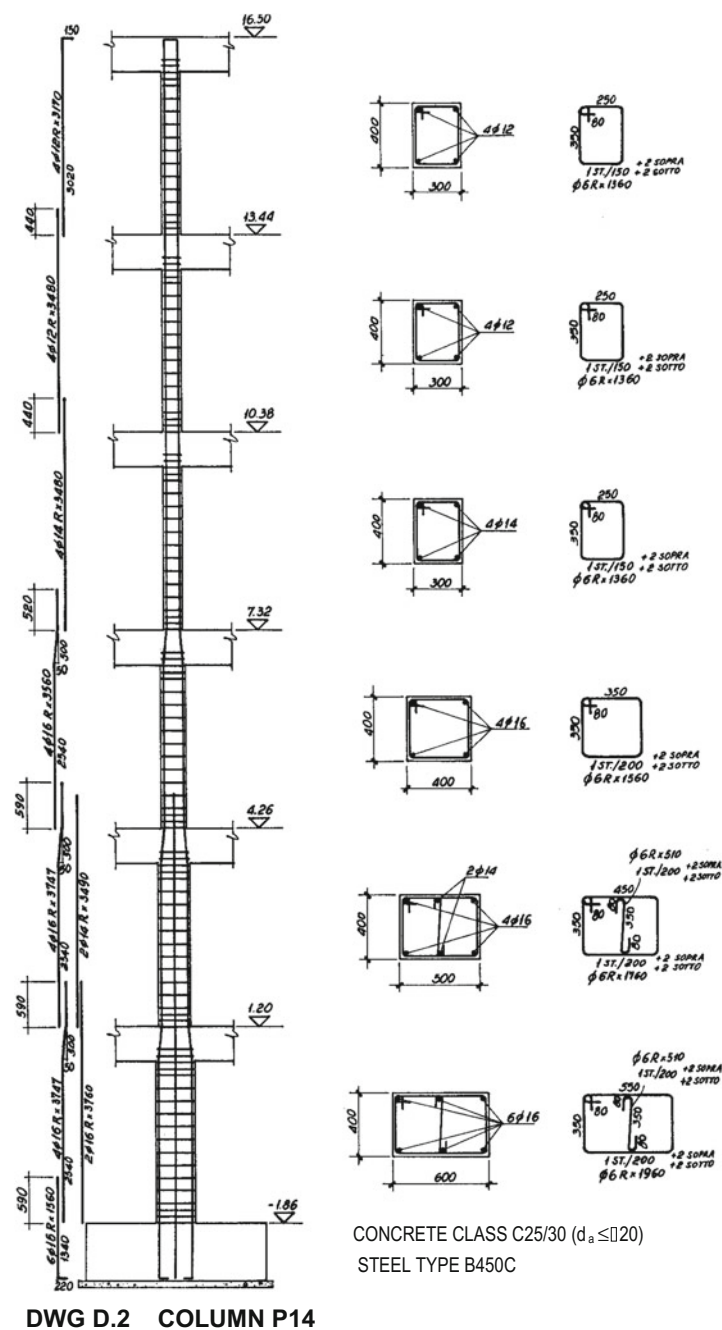


Fig. 2.24 Details of a column—elevation and sections

(see Table 1.7)

$$f_{ctd} = 1.95/1.5 = 1.30 \text{ N/mm}^2$$

$$f_{bd} = 2.25 \times 1.30 = 2.92 \text{ N/mm}^2$$

one obtains

$$l_b = \frac{\phi}{4} \frac{391}{2.92} \cong 33\phi$$

2.4.2 Notes on Reinforced Concrete Technology

Several construction requirements are shown as follows for the correct design of reinforced concrete structures. They are not exact compulsory rules; however, their general compliance is necessary to ensure that the models assumed in the design can actually correspond to the behaviour of the real structure.

Minimum Thicknesses

A first aspect concerns the minimum thicknesses to be assigned to elements in order to guarantee sufficient *homogeneity of the concrete*, also with respect to the relevance of the static function of the considered part. Such minimum thicknesses should be directly related to the maximum size d_a of the aggregate used that can vary for common structures between 12 and 25 mm. With the aim of ensuring a good distribution of grains up to $0.8d_a$ close to the maximum aggregate size, the following values can be indicated.

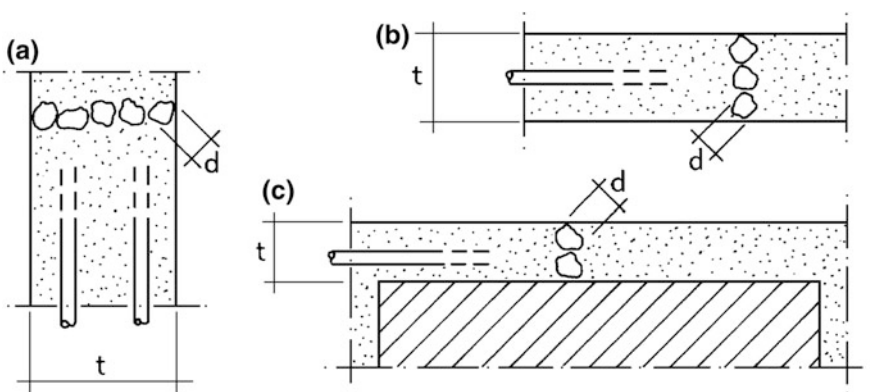


Fig. 2.25 Aggregate size and minimum thicknesses

- Structural elements reinforced on both faces (see Fig. 2.25a):

$$t \geq 0.8 \times 5d_a = 4.0d_a \quad (50-100 \text{ mm})$$

- Slabs and ribs with one layer of reinforcement (see Fig. 2.25b):

$$t \geq 0.8 \times 3d_a = 2.4d_a \quad (30-60 \text{ mm})$$

- Concrete collaborating toppings on permanent blocks (see Fig. 2.25c):

$$t \geq 0.8 \times 2d_a = 1.6d_a \quad (20-40 \text{ mm})$$

Given that the minimum size for a complete homogeneity of the material is equal to $5d_a$, in the structural parts with $t < 5d_a$ the characteristic concrete strength should be adequately reduced for design, for example with

$$f_{ck}^* = \left(0.5 + 0.1 \frac{t}{d_a} \right) f_{ck}$$

For plain (unreinforced) concrete elements the minimum thickness should be $t \geq 5.0d_a$.

In any case, an absolute minimum thickness value should be assigned, which derives from the type of material considered and from its processing technologies, in order to guarantee a *sufficient compact mass* to structural elements, for example with:

• components for extruded or vibrocompacted floors	$t \geq 30 \text{ mm}$
• ordinary cast in situ floor components	$t \geq 40 \text{ mm}$
• main structural elements	$t \geq 50 \text{ mm}$
• wall panels and plain concrete	$t \geq 80 \text{ mm}$

Bars Position

The position of bars in the cross section should respect minimum dimensions for spacing and edge distance. This is to allow aggregates to go through, to ensure a good concrete enclosure of the bars for bond purposes and also to ensure protection of the reinforcement against corrosion. The values given below to the *concrete cover* c and to the *bar spacing* i_h horizontal and i_v , vertical are measured to the centrelines of the bars (see Fig. 2.26); the *net cover* $c_o = c - \phi/2$ and the *net spacing* $i_o = i - \phi$ refer to the corresponding net thicknesses of concrete.

With the usual principle of allowing all (or almost) aggregate to go through, the following minimum dimensions can be indicated:

• Minimum net spacing:	horizontal i_{oh}	vertical i_{ov}
passive bars (see Fig. 2.26a)	$1.0 d_a$	$0.8 d_a$
prestressed strands (see Fig. 2.26b)	$1.2 d_a$	$1.0 d_a$

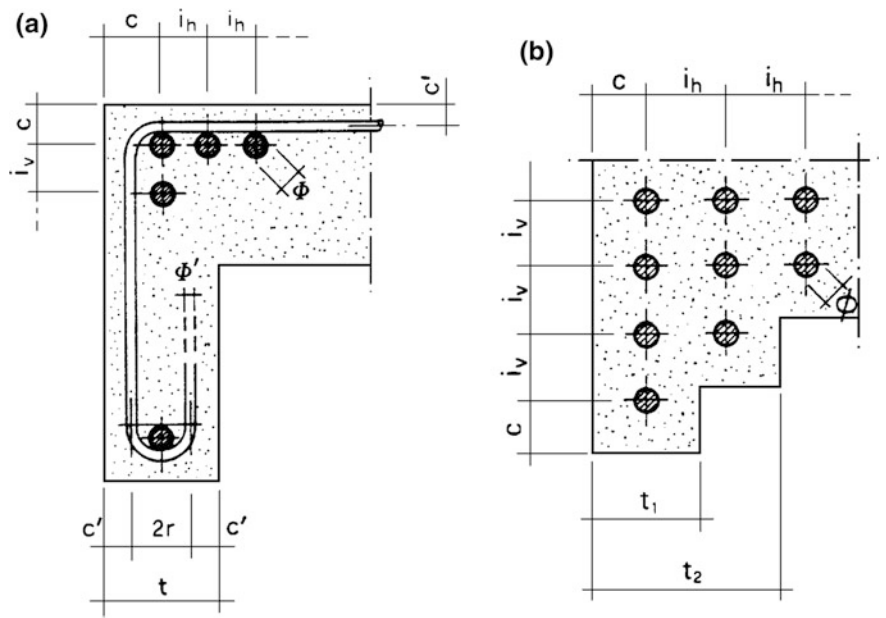


Fig. 2.26 Bar positioning—cover and spacing

• Minimum net cover:	c'_o	c_o
stirrups and links (see Fig. 2.26a)	$0.8 d_a$	—
passive reinforcement (see Fig. 2.26a)	—	$1.0 d_a$
prestressed reforc. (see Fig. 2.26b)	—	$1.0 d_a$

With the principle of ensuring a *good concrete enclosure of bars*, for a full bond due to a compact concrete layer around them, the following minimum dimensions can be indicated:

• Minimum values	spacing i_o	cover c_o
passive reinforcement (see Fig. 2.26a)	1.0ϕ	1.0ϕ
prestressed reforc. (see Fig. 2.26b)	2.0ϕ	1.5ϕ

With these values for example the thicknesses t_1 and t_2 of the prestressed element with adherent pretensioned strands indicated in Fig. 2.26b can be deduced. For strands of respectively 12.5 mm (0.5") and 15.2 mm (0.6"), one therefore has the following dimensions expressed in mm:

ϕ	i_o	c_o	$t_1 = 4\phi$	$t_2 = 7\phi$
12.5	25	19	50	88
15.2	30	23	61	106

In particular the thicknesses t_1 and t_2 shown here are compatible respectively with aggregates of $d_a \leq 12$, $d_a \leq 16$, $d_a \leq 20$ and $d_a \leq 25$ mm, except for possible increases due to the bending diameter of stirrups.

Concerning the cover necessary to ensure the *protection of reinforcement* against corrosion, one can refer to the following Sect. 2.4.3 where the problem of durability of reinforced concrete structures is discussed in more details.

It is implied that the greatest among the three requirements mentioned above has to be satisfied. An additional and more stringent cover requirement can be added when, because of the use conditions of the building, a particular *fire resistance* of structures is required. Moreover, it is to be kept in mind that an excessive cover causes problems with respect to cracking control. For values greater than the indicative value $c_o \cong 40$ mm, the addition of a *skin reinforcement* is generally required, not taken into account for resistance purposes, placed as protection of the outer layer for the normal service of structures.

Reinforcement Tolerances

The tolerances of execution and installation, related to the common production technology, lead to significant variability of dimensions with respect to the nominal values indicated in the design and therefore the minimum values shown above should be taken with due caution.

In particular, with reference to the *effects on structural safety*, the partial factors γ_M given by the codes already take into account the variability of resisting dimensions of the cross sections due to reinforcement tolerances. These tolerances are shown in Chart 2.5 of the Appendix.

With reference to the *effects on durability*, the tolerances of the concrete cover matter. This concrete cover has to be ensured with the use of adequate *spacers*, applied to the external bars of the reinforcement cage in order to impose the offset from the contiguous surface of the formwork. Table 2.17 of the Appendix takes into account such tolerances in giving the minimum values of cover for the different classes of exposure and resistance.

Bars Bending

In the design of sections and the reinforcement detailing, *bending radius* of bars also has to be taken into account, whose minimum value is related to the diameter of the bars in order to avoid microcracks during manufacturing. The value (see Fig. 2.27a)

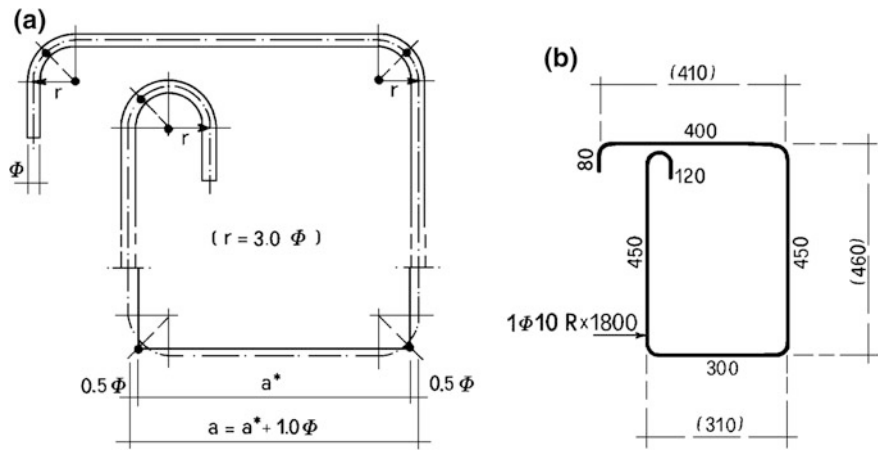


Fig. 2.27 Details of bar shaping

$$r \cong 3.0\phi$$

refers to ribbed bars that are nowadays commonly used. Such value refers to the axial circle; the internal bending diameter of the bar, corresponding to the one of the mandrel to be used, is equal to 5ϕ .

What mentioned above refers to the bending of longitudinal bars in order to obtain end hooks and also to the shaping of stirrups. For bent bars of beams, used as shear reinforcement in tension (see Chap. 5), the problem of possible cracking of concrete arises, caused by the compressions acting towards the inner part of the bend. In this case bending radii should be used that are roughly doubled.

In the *construction details drawings* the indications of radii are normally omitted (see Fig. 2.27b), limiting on giving the length of the axial polygon line of the bars, obviously in addition to their diameter and few additional dimensions if necessary. As indicated in details in Fig. 2.27a, the nominal side length a^* indicated in the drawing, equal to the development from end to end of the actual axial polygon line of the bar, is 1.0ϕ smaller than the actual dimension a of the bar.

It is to be noted that, in order to be inserted in the tool for bending, the end hook of a bar needs a certain extension beyond the circular bend. For the minimum length u , measured from the last end of the axial polygon line, the following values can be assumed in the detail drawings (see Fig. 2.27b):

• open (bend) at 90°	$u = 8\phi$
• semi-closed (hook) at 135°	$u = 10\phi$
• closed (loop) at 180°	$u = 12\phi$

The minimum thickness of a rib to be provided with stirrups as the one shown in Fig. 2.22a can now be deduced in the following way:

$$t \geq 2(c'_o + r) = 1.6d_a + 7\phi'$$

which, with the minimum commercial diameter of 6 mm, leads to 61 and 68 mm, respectively for aggregate sizes d_a equal to 12 and 16 mm. For bigger aggregates the limitation $t \geq 4.0d_a$ is the limiting one.

Reinforcement Anchorage

A very important aspect is the one related to the end anchorage of bars. As already mentioned at Sect. 1.4.3, in order to ensure the collaboration of the steel reinforcement in a given section it is necessary that the reinforcement be extended by a segment equal to the necessary *anchorage length*. According to the principle that ensures the full possible use of the resistance resources of steel everywhere, such length is obtained from

$$l_b = \frac{\phi f_{sd}}{4f_{bd}}$$

with $f_{bd} = \beta_b f_{ctd}$ and $\beta_b = 2.25$ for ribbed bars, $\beta_b \cong 1.0$ for smooth bars.

If instead one wants to refer to the actual stress acting in the bar, with a calculation repeated for each different situation, a reduced anchorage length can be attributed l'_b , estimated with the ratio between the required steel area and the one actually present:

$$l'_b = l_b A'_s / A_s$$

Such value refers to a bar in tension anchored inside a compact concrete zone. The same length can be conservatively assumed for the anchorage of bars in compression.

Bars interrupted in tensile zones and close to the external surface with the cover layer essentially ineffective for bond, would require a double anchorage length. They should be avoided, unless adequate confinement is provided with closely spaced transverse stirrups.

Reinforcement Joints

The problem of bars joints presents very similar problems. Excluding special techniques that are not very common, such as welding (allowed for steels explicitly indicated as weldable) or the use of couplers (threaded or sleeved), the reinforcement joint is obtained by simple *lapping* of the bars, adequately extended to ensure the anchorage of each of them.

Other than presenting once again the calculation of the anchorage length l_b recalled above, this joint requires the transfer of stresses from one bar to the other through the concrete around. The *bars distance* therefore has an influence on the lapping, according to what is indicated in Fig. 2.28a, whereas in Fig. 2.24b it is

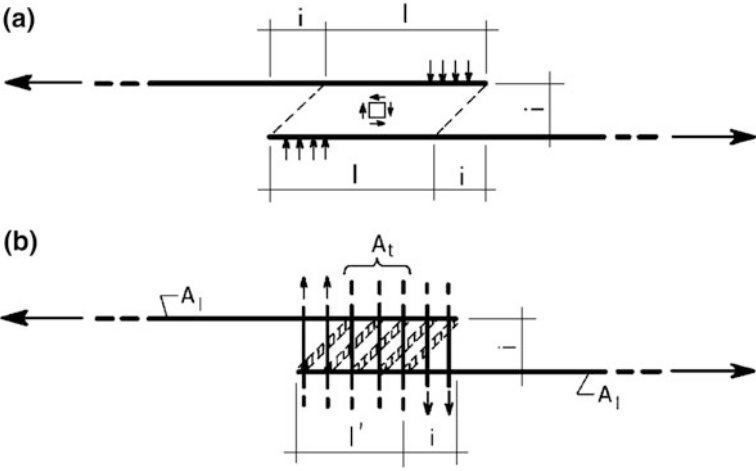


Fig. 2.28 Force transmission in bars overlapping zone

recalled how a good transverse confinement, with a total area of stirrups A_t equal to the one A_l of the reinforcement to be lapped, improves significantly the behaviour of the joint, letting concrete work only in compression in the resisting truss.

Transverse forces are also shown in Fig. 2.28, which are necessary to balance the offset tensions transferred between the longitudinal bars. Such forces are taken by the transverse stirrups in the case of Fig. 2.28b, whereas in the case of Fig. 2.28a

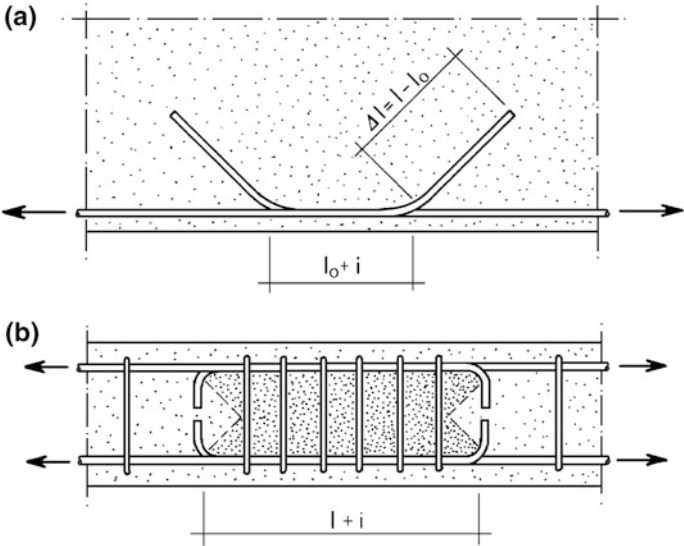


Fig. 2.29 Bars overlapping tension zones of beams (a) and ties (b)

they lead to tensions in the concrete in between. If not adequately designed, this type of joint can therefore lead to *longitudinal cracks* with opening of the joint.

The effectiveness of the anchorage, as already said, is reduced by the proximity of the reinforcement to the external surface and by the possible cracking state of concrete. Therefore, joints in tension zones are normally to be avoided and, when necessary, they should be staggered and provided with a segment $i + l_o$ of straight overlapping equal to at least $i + 20\phi$, followed by an end segment bent inwards, towards the compression zone (see Fig. 2.29a). The latter would have the extension Δl necessary to complete the required anchorage length l_b of the bar. In the design, the bond strength of the surface overlapping straight segment is to be halved.

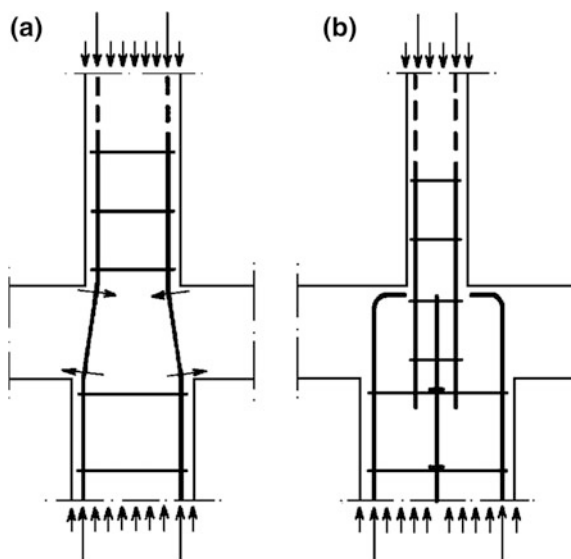
For ties with section fully in tension, lapping, when necessary, are to be designed with caution, evaluating the anchorage length with a halved bond strength and ending bars with additional hooks. The stirrups spacing should also be reduced locally, for a good *confinement of the joint*, creating a truss mechanism centred on the compression core of concrete (see Fig. 2.29b).

To conclude, it is to be noted how *fatigue phenomena* deriving from repeated loads can weaken bond, especially if under actions of alternate sign. This directly affects the effectiveness of anchorages and reinforcement joints.

Reinforcement Layout

A last aspect to be mentioned in these last pages refers to the reinforcement layout. In reinforced concrete, the steel bars have to resist axial forces mainly in tension. Their limited flexural stiffness, small with respect to the one of the composite element, causes that every *bar deviation* from the straight configuration concentrates transverse forces in concrete at the bending location.

Fig. 2.30 Details of bars overlapping in column joints



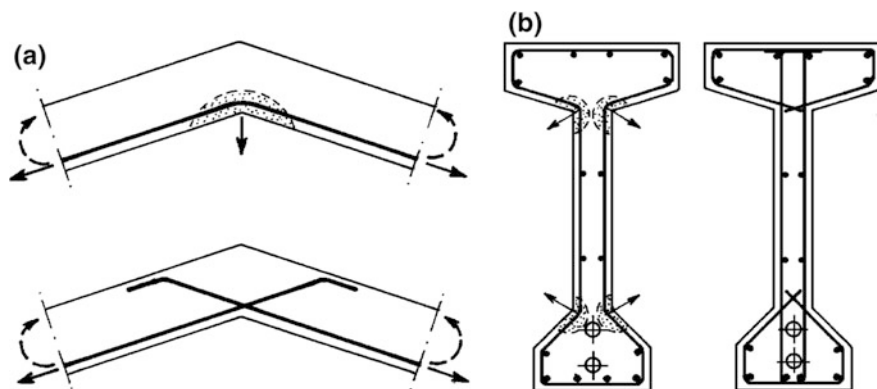


Fig. 2.31 Bad and good reinforcement details: knee beam (a) and PC section (b)

The case of elements in compression causes fewer concerns as the integrity of concrete allows the control of the diverging actions. As said before, the slenderness of the bars in compression should be limited with appropriate transverse bars (such as stirrups in column) to limit the tendency to buckle towards the outside, with possible spalling of concrete.

Figure 2.30a, b show instead the case of joints of superimposed segments of columns with different dimensions. Given that the sections are always fully in compression, if the angle of bending is small it is possible to redirect the longitudinal bars coming from the lower portion to insert them within the reduced area of the upper portion, allowing limited transverse forces contained within the deck thickness. Greater dimensional deviations require instead the interruption of the lower reinforcement and the start of the upper one with appropriate inner starter bars.

For reinforcement in tension, the problem is more delicate as it concerns zones of mostly cracked concrete, not capable of containing transverse diverging forces. In Fig. 2.31 two typical situations are described for example.

The first one refers to a folded beam in bending: in the incorrect solution shown on top, the transverse action of reinforcement in tension is indicated, which causes the spalling the concrete bottom; in the lower solution instead the reinforcement is correctly shaped, with straight extensions up to the compression zone and separate anchorages without transverse diverging forces.

Figure 2.31b refers to the I-section typical of precast beams in prestressed concrete. For the case of stirrups in tension, the incorrect solution which concentrates disruptive forces at the internal corners is indicated on the left side, the correct one that subdivides stirrups in three pieces and has every end side properly anchored with straight extensions on the right side.

2.4.3 *Durability Criteria of Reinforced Concrete Structures*

The durability aspects, which are discussed in the following pages, refer to structural elements in plain, reinforced and prestressed concrete. Only structures of common buildings, with residential, commercial or industrial use, as well as certain other civil construction, are considered.

The durability requirements refer to the resistance and serviceability of the structures as defined by the relative limit states in the appropriate structural verifications. Fire resistance is not considered; neither are other aspects such as insulation, appearance, etc....

In the following provisions, it has been assumed that fitting-out works and services be correctly executed and maintained in a good efficiency state, so to preserve structures from unexpected situations (water stagnation, overheating, damage of cover, leakage of aggressive materials, etc...).

Metallic inserts, even if connected or partially embedded in concrete elements, should be considered separately, with different criteria.

Service Life

The *expected service life* T_s is the period during which the structure is expected to maintain an adequate level of safety and functionality, without requiring excessive unexpected obligations for maintenance and repairs.

The capability of concrete structures to satisfy durability requirements is estimated through:

- the definition of the environmental conditions;
- the design provisions for materials and structures;
- the provisions for the execution and controls;
- the instructions for use and maintenance.

Apart from different provisions, explicitly indicated in the documentation of the design and contract, for common residential buildings the expected service life, exempt from excessive maintenance obligations, is assumed equal to 50 years.

Deterioration Processes

The following aggressive actions are considered:

- high presence of humidity;
- washout waters;
- marine environment;
- effects of freezing/thawing;
- chemical emissions.

Mechanical effects due to high stresses in materials are prevented with the verification of the specific serviceability limit states, such as the one of maximum compressions against progressive propagation of microcracking in concrete.

The physical deterioration due to abrasion is prevented with appropriate hard layers, such as the ones for carriage pavements.

The *presence of water* or humidity is the determining factor, which is directly connected to certain chemical reactions. It facilitates the flow of the other aggressive substances on the structures and determines their penetration inside concrete pores.

Under the actions listed above, the following deterioration processes are to be considered:

- the *corrosion of reinforcement* and of prestressing steel if directly exposed to oxidant agents or if exposed because of damages to the protective layer made of passive oxide when reached by carbonation of concrete cover, corrosion that develops with the progressive oxidation of steel, with expansions and spalling of concrete layers;
- the attack of concrete surface due to the direct *washout action* of rain or pure waters, possibly with carbon dioxide, which causes the dissolution of free unbonded lime and the progressive consumption of the material, or due to other surface processes of deterioration such as the expansion actions of sulphatic waters;
- chemical actions of *marine environment*, due to the high concentration of salts in environments submerged in water or in the saturated atmosphere of coastal areas, actions that develop with the surface dissolution caused by the expansion effects and that are increased in the splash zones because of the mechanical erosion of waves;
- the *freezing/thawing* effects due to the repeated formation of ice and increased by the use of antifreeze substances, effects that develop with the degradation of concrete caused by internal pressures of trapped water when freezes, and by spalling of the surface concrete caused by the high thermal gradient under the external antifreeze agents;
- other *chemical attacks* due to aggressive solids, liquids or gases, possibly facilitated by the presence of humidity.

Materials Properties

It is taken for granted that a correct technology is applied for the production of materials in order to avoid chemical instabilities, such as the alkali-aggregate reaction in concrete or the strain-age embrittlement of steel.

Concrete

With respect to durability a concrete of good quality is necessary in order to obtain:

- a *low permeability* to water penetration;
- a *well compacted* solid mass without enclosed voids;
- a homogeneous material of *high class* of resistance;
- a *skin without damages* with appropriate surface finishing.

For freeze-resistant concretes, a minimum air content (per unit mass of concrete) can be specified through the appropriate dosage of an air entraining admixture, to ensure a uniform distribution of micropores in which freezing water can freely expand.

Steel

The durability properties of steels for ordinary and prestressed reinforced concrete are related to the surface exposed per unit mass of the material, to the presence of surface cracks and their width.

These properties are given through a *sensitivity index* to corrosion that increases with

- small diameters of bars or strands;
- hardening processes of the material;
- high levels of tension in service states.

Reinforced concrete

Certain design criteria should be satisfied in order to obtain durable structures; first of all for any type of concrete structures the design should assume and explicitly indicate:

- the maximum size of the aggregate used in relation to the element thicknesses for a good homogeneity of the material and its consequent full strength;
- the minimum absolute value of thicknesses in order to ensure a overall sufficient mass of the elements;
- a proportioned choice of shapes and dimensions in order to avoid damages caused by early cracking due to shrinkage and thermal effects.

For reinforced concrete works, the design should add appropriate specifications regarding:

- the maximum aggregate size in relation to the free spaces between bars, and between bars and formwork in order to allow a complete compact cast of works;
- a minimum value of spacing between bars with reference to their diameters for a full bond resistance with concrete without damages at the interface;
- a minimum cover of reinforcement in relation to the concrete class and other factors that have an influence on steel corrosion.

Performances of Structures

The performances of the structures with respect to durability depend on the *service state* of the elements, which is related to the level of tensile stresses in concrete and which is distinguished in:

- *cracked state* when, under a rare load combination, the maximum tensile stress in concrete exceeds the characteristic strength βf_{ctk} ;

- *uncracked tension state* when, under the condition indicated above, the maximum tension, even if significant, does not exceed the characteristic value of the concrete strength βf_{ctk} ;
- *compression state* when, under the most unfavourable rare load combination, the concrete section remains entirely in compression.

The latter can be substituted by a less stringent one that limits the maximum tensile stress in concrete to a very conservative allowable value (for example $0.25\beta f_{\text{ctk}}$).

In the strength βf_{ctk} mentioned above it has to be assumed $\beta = 1$ for a constant distribution of tensions, $\beta = 1.3$ if referred to the extreme value of a triangular flexural distribution of stresses.

Also the type of *surface finishing* of elements should be considered distinguishing the cases of:

- elements with *exposed surfaces*, without any protection;
- *typical finishing*, such as plaster, tiling, ...;
- *special finishing*, with protective characteristics, such as waterproof barriers (membranes, water-repelling varnish, paints, ...);

where, for cracked states, varnish, paints or the other types of adherent coatings should be applied with special measures in order to preserve their integrity when the foreseen concrete cracking occurs.

Minimum Requirements

For *durable structures* certain minimum values of the relevant parameters should be fulfilled. In addition to the thicknesses of elements and the reinforcement spacing already mentioned in the previous paragraph, an additional geometric parameter relates to the different slenderness of the parts of an element: an excessive dimensional dissimilarity causes shrinkage and thermal effects that are highly differential, with the possibility of early cracking.

The following indicative prescription refers to the ratio between the equivalent thicknesses of the connected parts of the same concrete section:

Minimum shape ratio of the section:

$$\frac{s_1}{s_2} \geq \frac{1}{8} \quad (s_2 \geq s_1)$$

with $s_i = 2A_i/u_i$, where A_i is the area and u_i is the perimeter of the single homogeneous part of the cross section.

The main parameter related to the protection of reinforcement against corrosion is the concrete cover which can be given as a function of the aggressiveness of the environment and the material strength. The minimum values of cover are given in the table below, expressed in mm. They refer to constructions with a nominal life of 50 years. For constructions with a nominal life of 100 years (for example important bridges) they should be increased by 10 mm. For classes of resistance lower than

C_{min} they should be increased by 5 mm. For plate elements exposed to only one side they can be reduced by 5 mm.

Concrete classes		Environment	Bars for RC other elements		Strands other elements	
C_{min}	C_o	Aggressiveness	$C \geq C_o$	$C_{min} \leq C \leq C_o$	$C \geq C_o$	$C_{min} \leq C \leq C_o$
C25/30	C35/45	Low	20	25	20	25
C28/35	C40/50	Medium	30	35	30	35
C35/45	C45/55	High	40	45	40	45

The values of the table refer to actual built dimensions. In order to obtain the nominal values to be specified in the design, such values of cover should be increased by tolerances of reinforcement positioning assumed equal to ± 10 mm for ordinary workmanship, equal to ± 5 mm for controlled production. In any case it is implied that for the correct positioning, adequately distributed spacers are used. The indicative number is 4 per m^2 of formwork.

Appendix: General Aspects and Axial Force

Table 2.1: Environmental Conditions: Exposure Classes

The following table, reproduced in a summarized form, is extracted from the European Norm EN 206-1 “Concrete specification, performance, production and conformity”. Classes XC, XD and XS refer to corrosion of reinforcement, classes XF and XA refer to the surface attack of concrete.

Minimum concrete covers for the protection of reinforcement against corrosion for different degrees of aggressiveness are given in Table 2.17.

Class	Description	Examples
<i>1. No risk of corrosion or attack</i>		
X0	Plain concrete without attacks Reinf. concrete in very dry environ	Concrete inside buildings with very low air humidity
<i>2. Corrosion induced by carbonation</i>		
XC1	Dry or permanently wet	Concrete inside buildings
XC2	Wet, rarely dry	Many foundations
XC3	Moderate humidity	External concrete sheltered
XC4	Cyclic wet and dry	Structures in water line
<i>2. Corrosion induced by chlorides</i>		
XD1	Moderate humidity	Airborne salt
XD2	Wet, rarely dry	Swimming pools
XD3	Cyclic wet and dry	Bridges, outdoor pavements

(continued)

(continued)

Class	Description	Examples
<i>3. Corrosion induced by chlorides from sea water</i>		
XS1	Exposed to airborne salt	Structures near to the coast
XS2	Permanently submerged	Parts of marine structures
XS3	Tidal, splash and spray zones	Parts of marine structures
<i>4. Freeze/thaw attack</i>		
XF1	Wet surfaces, without de-icing agents	Vertical surf. exposed to rain
XF2	Wet surfaces, with de-icing agents	Vertical surfaces of bridges
XF3	Soaked surf. without de-icing agents	Horiz. surfaces open to rain
XF4	Soaked surf. with de-icing agents	Horiz. surfaces of bridges
<i>5. Chemical attack</i>		
XA1	Slightly aggressive chemical environ.	Natural soils-groundwater
XA2	Moderate aggressive chem. environ.	Natural soils-groundwater
XA3	Highly aggressive chemical environ.	Natural soils-groundwater

For design applications, with reference to corrosion of reinforcement, the exposure classes can be grouped as follows:

Aggressiveness	Exposure classes
Low	X0, XC1, XC2, XC3
Medium	XC4, XD1, XS1
High	XD2, XD3, XS2, XS3

With reference to freeze/thaw attack or chemical attack (classes XF and XA) an adequate concrete mix design should be adopted.

Chart 2.2: Concrete: Design Strength

In the resistance verifications (ultimate limit states) the following values (in MPa) are adopted:

$$f_{cd} = \alpha_{cc} \frac{f_{ck}}{\gamma_C} \quad \text{design compressive strength}$$

with $\alpha_{cc} = 1.00$ for short term loads and $\alpha_{cc} = 0.85$ for ordinary loads.

$$f_{c2} = 0.6 \left(1.0 - \frac{f_{ck}}{250} \right) f_{cd} \cong 0.50 f_{cd} \quad \text{reduced design strength}$$

$$f_{ctd} = \frac{f_{ctk}}{\gamma_C} \quad \text{tensile design strength}$$

where the partial safety factor should be assumed equal to:

$\gamma_C = 1.5$ for concrete of ordinary production

$\gamma_C = 1.4$ for concrete of controlled production with $\delta \leq 0.10$

(δ coefficient of variation = ratio of the standard deviation to the mean value).

In the verifications of stresses (serviceability limit state) the following values are adopted for concrete:

$\bar{\sigma}_c = 0.45 f_{ck}$ allowable tensile stress for quasi-permanent combination

$\bar{\sigma}_{cj} = 0.60 f_{ckj}$ allowable tensile stress for characteristic combination

$\bar{\sigma}'_{cj} = 0.70 f_{ckj}$ allowable tensile stress at prestressing.

The value of the ultimate tensile stress $\bar{\sigma}'_{ct} = \beta f_{ctk}$ refers to the limit of crack formation, with:

$\beta = 1.0$ for constant distribution

$\beta = 1.3$ for triangular distribution.

For parts with a thickness $t < 5d_a$, where d_a is the maximum aggregate size, all values of resistance and allowable stresses should be reduced by the factor $(0.5 + 0.1t/d_a)$.

Chart 2.3: Steel: Design Strength

In the resistance verifications (ultimate limit states) the values indicated below are adopted for steel of reinforced and prestressed concrete.

For passive reinforcement

$$f_{yd} = \frac{f_{yk}}{\gamma_S} \quad \text{design value of yield stress}$$

$$f_{td} = \frac{f_{tk}}{\gamma_S} (=k f_{yd}) \quad \text{design strength } (k = 1.20)$$

For prestressing reinforcement

$$f_{\text{ptd}} = \frac{f_{\text{ptk}}}{\gamma_s} \quad \text{design strength for prestressing strands}$$

$$f_{\text{ypd}} = 0.9f_{\text{ptd}} \quad \text{design value of the yield stress}$$

The partial safety factor for all reinforcements should be assumed equal to $\gamma_s = 1.15$.

In the verification of stresses (serviceability limit state) the values indicated as follows are adopted for steel.

For passive reinforcement

$$\bar{\sigma}_s = 0.80f_{yk} \quad \text{allowable stress of passive reinforcement}$$

For prestressing reinforcement

$$\bar{\sigma}_p = 0.80f_{pyk} \quad \text{allowable stress after losses}$$

$$\bar{\sigma}_{pi} = 0.85f_{pyk} \leq 0.75f_{ptk} \quad \text{initial admis. stress in post-tensioned tendons}$$

$$\bar{\sigma}_{pi} = 0.90f_{pyk} \leq 0.80f_{ptk} \quad \text{initial admis. stress in pre-tensioned tendons}$$

where f_{py} is to be substituted by $f_{p0.1}$ or f_{p1} , respectively for wires and strands.

In the calculations of stresses in service, the viscoelastic effects can be approximated with the assumption in the elastic formulas of

$$\alpha_e = \frac{E_s}{E_c} = 15$$

as homogeneization coefficient of the steel areas in the resisting section.

For tensile stresses in the reinforcement, the allowable limits given by Table 2.16 are also to be considered, for the cracking verifications.

Chart 2.4: Reinforcement: Shaping and Detailing

The schemes of the present chart refer to the bending of steel bars for reinforced concrete with a diameter $\phi \leq 24$ mm, unless noted otherwise.

- *Bending radius (at the axis)* for end hooks and stirrups:

$$r \geq 3.0 \phi$$

- *Mandrel diameter*

$$d_o = 2r - \phi \quad (\geq 5\phi)$$

- *Bending radius (at the axis)* for bent bars and continuous reinforcement

$$r' = 2r \quad (d'_o \geq 11\phi)$$

- *Developed length of the end hook* for $r = 3\phi$ with $\alpha = 90^\circ \div 135^\circ \div 180^\circ$ for bent bars and continuous reinforcement

$$u \geq 8\phi, 10\phi \text{ and } 12\phi$$

- *Detailing* referred to the rectified axial polygon line (with a^* nominal sides dimensioned in the reinforcement drawings)

$$a = a^* + 1.0\phi \quad \text{actual dimensions for } r = 5\phi$$

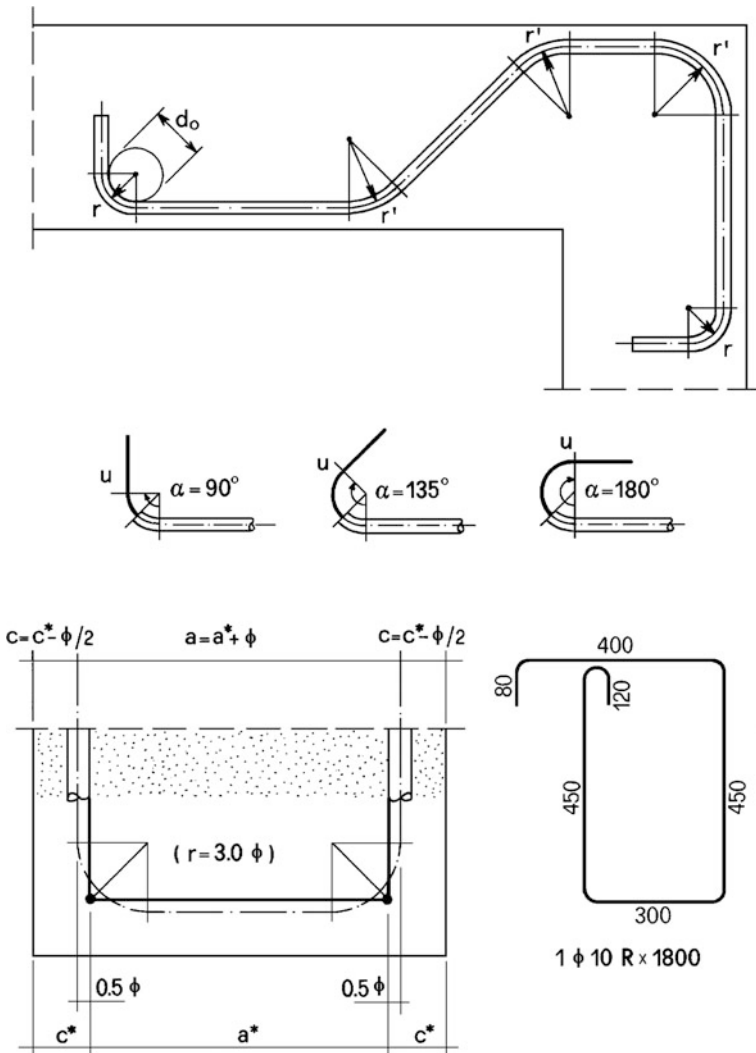


Chart 2.5: Reinforcement: Positioning Tolerances

The following deviations δ from the nominal dimensions shown in the design refer to the position of the longitudinal bars (passive bars or pretensioned strands) in the cross section. The relevant dimension (height or width) of the section is indicating with l .

$$\pm\bar{\delta} = 0.04 l (\geq 5 \text{ mm}) \text{ for } l < 500 \text{ mm}$$

$$\pm\bar{\delta} = 15 + 0.01 l (\leq 30 \text{ mm}) \text{ for } l > 500 \text{ mm}$$

The partial safety factors already take into account such tolerances in the resistance verifications.

For the values of cover, given that spacers adequately distributed on the form-work surfaces are used, it can be assumed:

$$\pm\delta = 10 \text{ mm}$$

The above-mentioned positioning tolerances can be halved in the case of industrial production in which the verification of bars positioning is part of the quality control system. In this case the tolerance of the cover becomes

$$\delta = -0 \quad \text{and} \quad \delta = +5 \text{ mm}$$

Table 2.6: Bond: Design Strength

The following table shows, for different codified classes of concrete and for the design of end anchorages of the bars, the following values:

f_{bk} characteristic bond strength

l_b anchorage length

Ordinary production $\Delta f = 8 \text{ MPa}$			Controlled production $\Delta f = 5 \text{ MPa}$		
Concrete class	f_{bk}	l_b/ϕ	Concrete class	f_{bk}	l_b/ϕ
			C30/37	5.2	28
C16/20	3.6	41	C35/43	5.6	26
C20/25	3.8	38	C40/50	6.1	24
C25/30	4.3	34	C45/55	6.5	22
C30/37	4.7	31	C50/60	7.0	21
C35/43	5.2	28	C55/67	7.4	20
C40/50	5.6	26	C60/75	7.6	19
C45/55	6.1	24	C70/85	8.1	18

The values are expressed in MPa and are deduced from the formulas:

$$f_{bk} = \beta_b f_{ctk} \text{ (see Table 1.2)}$$

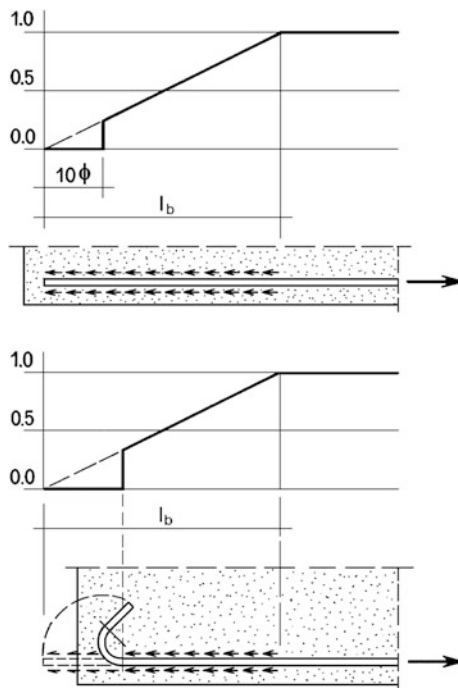
$$\beta_b = 2.25 \text{ for ribbed bars}$$

$$l_b = \frac{\phi f_{yd}}{4 f_{bd}} \quad (f_{yd} = f_{yk} / \gamma_s; f_{bd} = f_{bk} / \gamma_c)$$

In particular, the anchorage length refers to the ribbed bars in steel of the type B450C, with $\gamma_s = 1.15$ and $\gamma_c = 1.5$ and it is expressed as a ratio to the diameter ϕ of the bar (l_b/ϕ). For anchorages in surface zones in tension, the bond strength should be halved.

Chart 2.7: Reinforcement: Anchorages and Overlaps

It can be assumed that bond stresses at the end of a bar in tension are distributed along the anchorage length l_b with a constant value and that the effectiveness of the bar in tension increases linearly starting from its end up to the full value ($=1.0$) of its capacity, reached at the distance l_b . The first segment equal to 10ϕ is to be considered ineffective. For the anchorage, hooks are to be calculated with reference to their developed length and they are to be considered ineffective up to the tangent point. The following scheme refers to an end anchorage in uncracked zone.



The overlapping on the tension side corresponds to a double end anchorage of the consecutive bars and it should be done with a segment $l_b < (20\phi + i)$ of straight overlapping, where i is the distance between bars to be joint, plus an end segment of length $u \geq 10\phi$ bent inwards, towards the compression zone. For bond, the effectiveness of the surface straight segment l_{ob} should be halved; the full capacity of the bar is therefore reached at:

$$l_{ob} = 2(l_b - u)$$

with l_b defined in Table 2.6. The following scheme gives the complementary growth of the effectiveness of the two joint bars. The capacity of the joint, indicated by the dotted line, can be enhanced increasing the overlapping.

Reinforcement joints in tie elements should be done with a full confinement, introducing transverse stirrups in the segment of bars overlapping, commensurate to the axial force to be transferred.

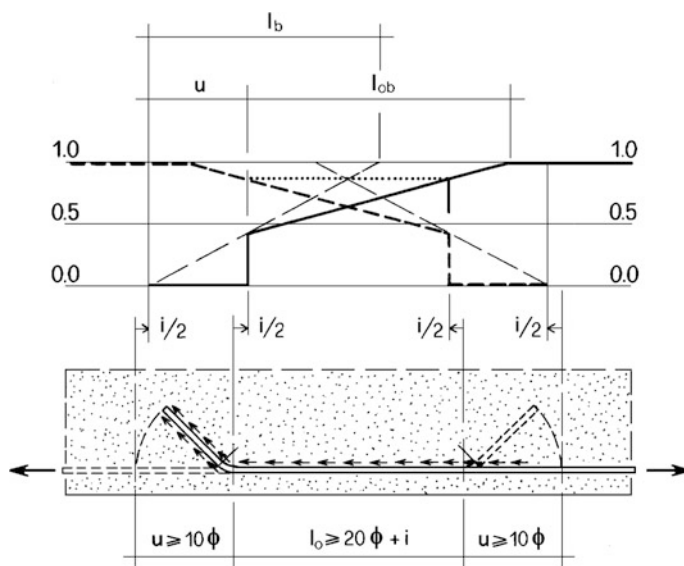


Chart 2.8: Concrete Structures: Minimum Dimensions

Structural elements in plain, reinforced and prestressed concrete should be designed with the minimum dimensions given by the most restrictive minimum values of the following cases:

Absolute Minimum Thicknesses

Technological limits to ensure a *sufficient compact mass*:

components for extruded or vibrocompacted floors	$t \geq 30 \text{ mm}$
components for cast in situ floors	$t \geq 40 \text{ mm}$
parts of main structural elements	$t \geq 50 \text{ mm}$
wall panels and plain concrete	$t \geq 80 \text{ mm}$

Relative Minimum Thicknesses

Requirement of good *homogeneity of concrete* for a uniform strength (d_a = maximum aggregate size):

• walls in plain concrete (unreinforced)	$t \geq 5.0 d_a$
• structural elements reinforced on both sides	$t \geq 4.0 d_a$
• slabs and ribs reinforced on one layer	$t \geq 2.4 d_a$
• reinforced toppings sitting on permanent blocks	$t \geq 1.6 d_a$

Minimum Bar Spacing (Concrete)

Guarantee of the passage of aggregates for good compaction of concrete (d_a = maximum aggregate size):

	Spacing		Cover
	Horizontal i_{oh}	Vertical i_{ov}	c_o
• stirrups and links	$\geq 1.6 d_a$	$\geq 1.6 d_a$	$\geq 0.8 d_a$
• passive reinforcement	$\geq 1.0 d_a$	$\geq 0.8 d_a$	$\geq 1.0 d_a$
• pretensioned reforc.	$\geq 1.2 d_a$	$\geq 1.0 d_a$	$\geq 1.0 d_a$

Minimum Bar Spacing (Steel)

Requirement of *good encasing* of bars for effective bond (ϕ reinforcement diameter):

	Spacing i_o	Cover c_o
• passive reinforcement	$\geq 1.0 \phi$	$\geq 1.0 \phi$
• pretensioned reforc.	$\geq 2.0 \phi$	$\geq 1.5 \phi$

For cover see also Table [2.17](#).

Chart 2.9: Ordinary Columns: Formulas and Construction Rules

Reinforced concrete sections subject to compression axial force.

Symbols

N_{Ek}	characteristic axial force
N_{Ed}	design axial force
b	smaller side dimension of section
ϕ	diameter of longitudinal bars
ϕ'	stirrups diameter
i	centre-to-centre distance of longitudinal bars
s	stirrups spacing (current part)
s'	stirrups spacing (column ends)
A_c	concrete area
A_s	area of longitudinal reinforcement
$\rho_s = A_s/A_c$	geometrical reinforcement ratio
$\alpha_e = E_s/E_c$	elastic moduli ratio (see Chart 2.3)
$\psi_s = \alpha_e \rho_s$	elastic reinforcement ratio
f_{cd}	concrete design strength
f_{yd}	reinforcement design strength
$r_s = f_{yd}/f_{cd}$	design strength ratio
$\omega_s = r_s \rho_s$	mechanical reinforcement ratio
σ_c	concrete stress
σ_s	steel stress
$\bar{\sigma}_c$	concrete allowable stress (see Chart 2.2)
N_{Rd}	design resisting axial force

Verifications

Service

$$\sigma_c = \frac{N_{Ed}}{A_c(1+\psi_s)} \leq 0.7\bar{\sigma}_c \quad (\sigma_s = \alpha_e \sigma_c)$$

Resistance

$$N_{Rd} = f_{cd}A_c(0.8 + \bar{\omega}_s)$$

Construction requirements

$b \geq 200 \text{ mm}$	($\geq 150 \text{ mm}$ in prefabrication)
$A_s \geq 0.10 N_{Ed}/f_{yd}$	$i \leq 300 \text{ mm}$
$\rho_s \geq 0.003$	$s \leq b$
$\rho_s \leq 0.04$	$s \leq 300 \text{ mm}$

$$\begin{aligned}\phi &\geq 12 \text{ mm} & s &\leq 12 \phi \\ \phi' &\geq \phi / 4 & s' &\leq 0.6 s\end{aligned}$$

Chart 2.10: Confined Columns: Formulas and Construction Requirements

Symbols

D	diameter of spiral
n	number longitudinal bars
s	pitch of spiral or spacing of hoops
a_w	area of spiral or hoops
$A_n = \pi D^2/4$	area of confined core
$A_w = a_w \pi D/s$	equivalent area of spiral or hoops
$\omega_1 = r_s A_1/A_n$	longitudinal mechanical reinforcement ratio
$\omega_w = r_s A_w/A_n$	spiral or hoops mechanical reinforcement ratio

See also Chart 2.9.

Verifications

Service

$$\sigma_c = \frac{N_{Ed}}{A_c(1+\psi_s)} \leq \bar{\sigma}_c \quad (\sigma_s = \alpha_e \sigma_c)$$

Resistance

$$N_{Rd} = f_{cd} A_c (0.8 + \omega_1 + 1.6 \omega_w) \geq N_{Ed}$$

Construction Requirements

$$n \geq 6$$

$$s \leq D/5$$

$$0.8 + \omega_1 + 1.6 \omega_w \leq 2$$

$$A_1 \geq A_w/2$$

Data of Chart 2.9 are also valid except s' .

Chart 2.11: RC Walls: Construction Requirements

Walls reinforced on both sides with internal vertical bars and external horizontal bars.

Symbols

t	wall thickness
ϕ	diameter of vertical bars
ϕ'	diameter of horizontal bars
i	centre-to-centre distance between vertical bars
s	spacing of horizontal bars
c	edge axis distance
a_v	area of vertical reinforcement per unit length
a_h	area of horizontal reinforcement per unit height

Construction requirements

$a_v \geq 0.0030 t$	(total on both sides)
$a_v \leq 0.04 t$	(total on both sides)
$a_h \geq 0.0015 t$	(total on both sides) $i \leq 300 \text{ mm}$
$\phi \geq 8 \text{ mm}$	$i \leq 2 t$
$\phi' \geq \phi/3$	$s \leq 300 \text{ mm}$
$c \geq 2 \phi$	$s \leq 25 \phi$

The end parts of the walls are to be reinforced with longitudinal (vertical) and transverse bars according to the requirements for ϕ , ϕ' and s of Chart 2.9.

The requirements above are to be applied if the vertical reinforcement is taken into account in the calculation of the capacity of the wall according to the verification formulas of Chart 2.9.

Table 2.12: Creep in Columns: Stress Redistribution

The following table shows, for different elastic reinforcement ratios and for the three nominal coefficients of final creep given for RC in Table 1.16, the stress variation ratios with respect to the initial elastic values:

ψ_s	$\varphi_\infty = 1.9$			$\varphi_\infty = 2.5$			$\varphi_\infty = 3.1$		
	α_e^*	σ_c^*	σ_s^*	α_e^*	σ_c^*	σ_s^*	α_e^*	σ_c^*	σ_s^*
0.00	2.90	1.00	2.90	3.50	1.00	3.50	4.10	1.00	4.10
0.02	2.94	0.96	2.83	3.56	0.95	3.39	4.20	0.94	3.95
0.04	2.97	0.93	2.76	3.62	0.91	3.29	4.29	0.89	3.81
0.06	3.01	0.90	2.70	3.69	0.87	3.20	4.39	0.84	3.68
0.08	3.04	0.87	2.64	3.75	0.83	3.11	4.48	0.79	3.56
0.10	3.07	0.84	2.59	3.81	0.80	3.03	4.58	0.75	3.46
0.12	3.11	0.82	2.53	3.87	0.77	2.96	4.68	0.72	3.36
0.14	3.14	0.79	2.49	3.93	0.74	2.89	4.77	0.68	3.26
0.16	3.17	0.77	2.44	3.99	0.71	2.82	4.87	0.65	3.17

(continued)

(continued)

ψ_s	$\varphi_\infty = 1.9$			$\varphi_\infty = 2.5$			$\varphi_\infty = 3.1$		
	α_e^*	σ_c^*	σ_s^*	α_e^*	σ_c^*	σ_s^*	α_e^*	σ_c^*	σ_s^*
0.18	3.20	0.75	2.40	4.04	0.68	2.76	4.96	0.62	3.09
0.20	3.24	0.73	2.36	4.10	0.66	2.70	5.06	0.60	3.02
0.22	3.27	0.71	2.32	4.16	0.64	2.65	5.15	0.57	2.95
0.24	3.30	0.69	2.28	4.22	0.62	2.60	5.25	0.55	2.88
0.26	3.33	0.68	2.25	4.27	0.60	2.55	5.34	0.53	2.82
0.28	3.36	0.66	2.21	4.33	0.58	2.50	5.44	0.51	2.76
0.30	3.38	0.65	2.18	4.38	0.56	2.46	5.53	0.49	2.70
0.32	3.41	0.63	2.15	4.44	0.55	2.42	5.62	0.47	2.65
0.34	3.44	0.62	2.13	4.49	0.53	2.38	5.71	0.46	2.60
0.36	3.47	0.60	2.10	4.54	0.52	2.34	5.80	0.44	2.56
0.38	3.50	0.59	2.07	4.60	0.50	2.31	5.90	0.43	2.51
0.40	3.52	0.58	2.05	4.65	0.49	2.28	5.99	0.41	2.47

$\alpha_e^* = \alpha_{e\infty}/\alpha_e$ homogeneization coefficient of reinforcement

$\sigma_c^* = \sigma_{c\infty}/\sigma_{c0}$ final stress in concrete

$\sigma_s^* = \sigma_{s\infty}/\sigma_{s0}$ final stress in steel ($=\varepsilon_\infty/\varepsilon_0$)

where the stresses σ_{c0} , σ_{s0} in the materials are intended to be calculated with the service verification formula of Chart 2.9 based on the actual ratio $\alpha_e = E_s/E_c$ of elastic moduli.

The values of the table are calculated with the formulas:

$$\alpha_e^* = \frac{e^{\beta\phi_\infty}}{\beta} - \frac{1}{\psi_s} \quad \text{with } \beta = \frac{\psi_s}{1 + \psi_s}$$

$$\sigma_c^* = e^{-\beta\phi_\infty}$$

$$\sigma_s^* = \alpha_e^* \sigma_c^*$$

valid for concrete loaded at an early stage (extreme ageing theory).

Table 2.13: Shrinkage in RC: Stress Effects

The following table shows, for the different elastic reinforcement ratios $\psi_s = \alpha_e \rho_s$, the coefficients

$$\beta = \frac{\psi_s}{1 + \psi_s} \quad \beta' = \frac{1}{1 + \psi_s}$$

for the calculation of shrinkage self-induced stresses in concrete and steel

$$\sigma_{cs} = \beta \sigma_{ce} \quad \sigma_{ss} = -\beta' \sigma_{se}$$

with

$$\sigma_{ce} = E_c \varepsilon_{cs} \quad \sigma_{se} = E_s \varepsilon_{cs}$$

in the doubly symmetric RC sections (ε_{cs} = concrete shrinkage).

ψ_s	β	β'	ψ_s	β	β'
0.00	0.00	1.00			
0.02	0.02	0.98	0.22	0.18	0.82
0.04	0.04	0.96	0.24	0.19	0.81
0.06	0.06	0.94	0.26	0.21	0.79
0.08	0.07	0.93	0.28	0.22	0.78
0.10	0.09	0.91	0.30	0.23	0.77
0.12	0.11	0.89	0.32	0.25	0.76
0.14	0.12	0.88	0.34	0.25	0.75
0.16	0.14	0.86	0.36	0.26	0.74
0.18	0.15	0.85	0.38	0.28	0.72
0.20	0.17	0.83	0.40	0.29	0.71
			∞	1.00	0.00

Chart 2.14: Ties in Reinforced and Prestressed Concrete

Reinforced concrete sections subject to axial tension force with possible centred precompression.

Symbols

A_p	area of prestressing reinforcement
$\rho_p = A_p/A_c$	geometric prestressing reinforcement ratio
$\psi_p = \alpha_e \rho_p$	prestressing elastic reinforcement ratio
$A_t = A_s + A_p$	total area of passive plus active reinforcement
$\psi_t = \psi_s + \psi_p$	total elastic reinforcement ratio
$\alpha = A_s/A_p$	passive to active reinforcement ratio
σ_{po}	prestressing stress in the tendon
$N_{po} = \sigma_{po} A_p$	prestressing force in the tendon

See also Charts 2.2, 2.3 and 2.9.

Verifications

Service

- *Uncracked section*

$$\sigma_c = \frac{N_{ak} - N_{po}}{A_c(1 + \psi_t)}$$

$$\sigma_s = \alpha_e \sigma_c \quad \sigma_p = \alpha_e \sigma_c + \sigma_{po}$$

Verification of decompression of concrete $\sigma_c \leq 0$

Verification of cracks formation $\sigma_c \leq \bar{\sigma}'_{ct}$

- *Cracked section*

$$\sigma_s = \frac{N_{ak} - N_{po}}{A_t} \leq \bar{\sigma}_s \text{ (see also Table 2.16)}$$

$$\sigma_p = \frac{N_{ak} - \alpha N_{po}}{A_t} \leq \bar{\sigma}_s \text{ (see also Table 2.16)}$$

Resistance

$$N_{Rd} = f_{sd}A_s + f_{pd}A_p \geq N_{ad}$$

Minimum reinforcement

$$A_s \geq A_c f_{ctm} / f_{yk}$$

For technological data see Chart 2.15.

Chart 2.15: Cracking in RC and PC: Verification Scheme

The following scheme shows the verifications required in the different service conditions of the elements in reinforced and prestressed concrete. The symbols are defined here under:

σ'_s stress in passive reinforcement calculated in the cracked section;
 σ_c stress in concrete in tension calculated in the uncracked section;
 $\sigma_p^* = \sigma'_p - \sigma_{po}$ stress increment in the pretensioned reinforcement calculated in the cracked section with respect to the decompression of concrete;

Type of reinforce	Load combinations	Environment aggressiveness		
		Low	Medium	High
Passive	Rare	–	–	–
	Frequent	$\sigma'_s \leq \bar{\sigma}'_{s3}$	$\sigma'_s \leq \bar{\sigma}'_{s2}$	$\sigma'_s \leq \bar{\sigma}'_{s1}$
	Quasi perman.	$\sigma'_s \leq \bar{\sigma}'_{s2}$	$\sigma'_s \leq \bar{\sigma}'_{s1}$	$\sigma'_s \leq \bar{\sigma}'_s$
Pretensioned	Rare	–	$\sigma_C < \beta f_{ctk}$	$\sigma_C < \beta f_{ctk}$
	Frequent	$\sigma_p^* \leq \bar{\sigma}'_{s2}$	$\sigma_p^* \leq \bar{\sigma}'_{s1}$	$\sigma_p^* \leq \bar{\sigma}'_s$
	Quasi perman.	$\sigma_p^* \leq \bar{\sigma}'_{s1}$	$\sigma_p^* \leq \bar{\sigma}'_s$	$\sigma_C \leq 0$

For the allowable stresses $\bar{\sigma}'_{s1}$, $\bar{\sigma}'_{s2}$, $\bar{\sigma}'_{s3}$, see Table 2.16. The passive reinforcement is made of ribbed bars; the pretensioned reinforcement is made of adherent smooth or indented wires or strands. For the classification of environments see Table 2.1.

- $\bar{\sigma}'_s = 0.5\sigma'_{sr}$
- with σ'_{sr} stress corresponding to cracking of the section ($\bar{\sigma}_{sr} = (A_c + \alpha_c A_s)f_{ctk}/A_s$ for ties);
- $\beta f'_{ctk}$
- characteristic tensile strength of concrete (with $\beta = 1.0$ for constant distribution and $\beta = 1.3$ for triangular distribution of stresses);
- $\sigma_D^* = \sigma'_D - \sigma_{DO}$
- increment of tension in pretensioned reinforcement calculated in the cracked section with respect to decompression in concrete.

Table 2.16: Cracking in RC and PC: Allowable Stresses

The following table shows, for different values of the diameter ϕ , the allowable stresses in passive and pretensioned reinforcement to be used in cracking verifications of Chart 2.15. Stresses $\bar{\sigma}'_{s1}$, $\bar{\sigma}'_{s2}$, $\bar{\sigma}'_{s3}$ correspond respectively to crack widths $\bar{w}_1 = 0.2$ mm, $\bar{w}_2 = 0.3$ mm, $\bar{w}_3 = 0.4$ mm.

The values are expressed in MPa and refer to longitudinal reinforcement with ribbed bars distributed along the edges in tension of the section, with a centre-to-centre distance

- $i \leq 5\phi$ for pure tension (ties)
- $i \leq 8\phi$ for pure bending (beams)

and to alternate or long duration loads.

Pure tension (Ties)			ϕ (mm)	Pure bending (beams)		
$\bar{\sigma}'_{s1}$	$\bar{\sigma}'_{s2}$	$\bar{\sigma}'_{s3}$		$\bar{\sigma}'_{s1}$	$\bar{\sigma}'_{s2}$	$\bar{\sigma}'_{s3}$
240	320	360	8	280	360	400
225	280	320	10	260	320	360
210	250	290	12	240	280	320
195	235	295	14	220	260	300
180	220	260	16	200	240	280
165	205	235	18	190	230	260
150	190	210	20	180	220	240
140	175	190	22	170	210	230
130	165	180	24	160	200	220

This table is deduced from the analogous table of the standard EN 1992-1-1:2004 with adequate adaptations.

Table 2.17: Durability: Minimum Cover of Reinforcement

The following tables give, for the different combination of environmental aggressiveness (see Table 2.1), the values of minimum reinforcement cover for the protection against corrosion. The values of the table are expressed in mm and refers to the actual concrete cover required for constructions of a nominal life of 50 years. The nominal values of cover to be shown in the drawings would have to be increased by the positioning tolerances of reinforcement assumed equal to ± 10 mm for ordinary production, equal to ± 5 mm for controlled production.

Concrete classes		Environment	Bars for plate elements		Bars for other elements	
C_{\min}	C_o	Aggressiv.	$C \geq C_o$	$C_{\min} \leq C < C_o$	$C \geq C_o$	$C_{\min} \leq C < C_o$
C25/30	C35/45	Low	15	20	20	25
C30/37	C40/50	Medium	25	30	30	35
C35/45	C45/55	High	35	40	40	45

Concrete classes		Environment	Strands for plate elements		Strands for other elements	
C_{\min}	C_o	Aggressiv.	$C \geq C_o$	$C_{\min} \leq C < C_o$	$C \geq C_o$	$C_{\min} \leq C < C_o$
C25/30	C35/45	Low	25	30	30	35
C30/37	C40/50	Medium	35	40	40	45
C35/45	C45/55	High	45	50	50	50

For constructions with a nominal life of 100 years, the values of the table should be increased by 10 mm. For strength classes lower than C_{\min} , such values are to be increased by 5 mm. For elements of controlled production they can be reduced by 5 mm.

Reinforced Concrete Design to Eurocode 2

Toniolo, G.; di Prisco, M.

2017, XXVII, 836 p. 448 illus., Hardcover

ISBN: 978-3-319-52032-2